UNIVERSITÀ DEGLI STUDI DI PADOVA

Dipartimento di Ingegneria Industriale DII

Corso di Laurea Magistrale in Ingegneria Aerospaziale

Characterization of in-orbit catastrophic fragmentations

Relatore: Olivieri Lorenzo

Minato Marco 2053141

Anno Accademico 2022/2023

Summary

Since the dawn of space exploration, near-Earth space has progressively become more populated with man-made inactive objects, including fragments. These objects, collectively referred to as space debris, can range from small particles to large structures, presenting a significant challenge to the safety of future space missions. A single breakup event alone can lead to a substantial increase in the number of fragments within Earth's orbit, consequently elevating the risk of collisions between space debris and operational satellites. This thesis delves into the phenomenon of in-orbit catastrophic fragmentations, conducting a comprehensive analysis of existing models and providing a definition of "catastrophic breakup" based on observed historical data. It also explores failure modes that could be included in the given definition, with a specific focus on their impact on the space debris environment. Following this, a case study is carried out to assess the probability of a catastrophic breakup occurring under the defined thresholds, while also examining potential mitigation strategies. This research aims to contribute to a deeper understanding of the space debris environment, offering fresh perspectives on how to address this intricate challenge within the field of aerospace engineering.

Contents

List of Figures

Chapter 1

Introduction

Orbiting satellites are indispensable in our modern world, playing a crucial role in numerous domains and disciplines. These include telecommunications, meteorology, navigation, Earth monitoring, climate research, space science, and research, all while acknowledging their pioneering contributions to the inception of human space exploration. Satellites offer an unmatched vantage point, serving as invaluable tools for collecting scientific data, promoting commercial ventures, and facilitating a diverse range of vital applications and services. Consequently, they unlock unparalleled opportunities for both research and the practical utilization of these technological assets. In more than 60 years of space exploration, more than 6000 launches have occurred, and in the last decades, space debris started to hazard operational satellites [1].

Space debris are any human-made object in Earth orbit that are non functional, they size from old spacecraft and the rocket stages that launched them to micro-debris like flecks of paint. Every object launched in orbit can be a potential source of space debris, which circle at speeds of approximately 7 to 8 km/s in Low Earth Orbit (LEO). However, the average impact speed of orbital debris with another space object is approximately 10 km/s, which roughly ten times the speed of a bullet. Consequently, collisions with even a small piece of debris will involve significant energy and cause the production of even more space debris escalating the collision rate. This phenomenon is

commonly referred to as the "Kessler Syndrome".

While the term "Kessler Syndrome" has sometimes been sensationalized by the media, the orbital debris environment is increasingly shaped by chance collisions, shifting away from its previous dominance by explosion events [2].

1.1 The origin of space debris

The launch of Sputnik I in 1957 not only marked the inception of human space exploration but also heralded the birth of human-made orbital debris. This included the rocket stage that launched the artificial satellite and the satellite itself. It also underscored the imperative need to monitor these objects in space. This awareness led to the establishment of Project Space Track by the United States Air Force, a comprehensive system designed to track artificial space objects, regardless of their foreign or domestic origins.

Subsequent and concerted efforts were launched to maintain the tracking of spacecraft. One prominent initiative was the creation of the Space Object Catalog, meticulously managed by the North American Aerospace Defense Command (NORAD). This catalog aimed to provide a detailed inventory of space objects, enhancing our ability to monitor and understand the ever-evolving space environment.

On a significant date, June 29, 1961, an incident occurred that marked a pivotal moment in space history. A Thor-Ablestar rocket upper stage experienced a catastrophic explosion, resulting in what is now recognized as the first-ever satellite breakup event. This incident generated more than 200 cataloged fragments, a startling testament to the potential hazards posed by space debris. Over the ensuing years, the number of cataloged space debris items continued to rise steadily. Additionally, smaller fragments that eluded precise tracking contributed to the growing challenge of managing the space debris population, underscoring the importance of continued vigilance and research in this critical area.

1.2 Tracking capabilities

Not all space debris are visible from the ground. Some objects are too small to be observed, while others evade tracking due to their specific orbits. Measurements of orbital debris are carried out through a combination of ground-based and space-based observations within the orbital debris environment.

This comprehensive data is collected using various methods, including ground-based radars, optical telescopes, space-based sensors, the analysis of surfaces retrieved from spacecraft that have ventured into space, and controlled experiments conducted in terrestrial laboratories. Prominent data sources that have played a pivotal role in this undertaking encompass the U.S. Space Surveillance Network (SSN), the Haystack X-Band Radar, and materials retrieved from missions such as Solar Max, the Long Duration Exposure Facility (LDEF), the Hubble Space Telescope (HST), and the Space Shuttle. In general, radar measurements have found utility in tracking objects at lower altitudes, while optical measurements have been effective for monitoring orbits at higher altitudes. In the case of extremely small debris, on-site measurements, such as the examination of surfaces retrieved from spacecraft, become a valuable resource.

The majority of catalogued objects, which are typically tracked by the U.S. SSN as depicted in Figure 1.1, fall under a specific size threshold. In LEO, catalogued debris is generally considered to be larger than 10 cm in diameter, while at higher altitudes, the threshold is set at 1 m. Debris catalogued due to fragmentations occurring in Molniya-type orbits (which are highly elliptical with 63° inclination) are usually low, in part due to stable perigees situated deep in the Southern Hemisphere and often beyond SSN coverage [3].

A "catalogued object" refers to an object that has been meticulously recorded and documented within a well-organized catalog. This catalog contains crucial information about the object's orbital elements, including its semi-major axis, eccentricity, inclination, perigee height, and apogee height. These catalogued objects undergo continuous tracking and monitoring to ensure their

positions remain known and predictable. Each object is assigned a unique identifier and receives regular updates in the catalog to facilitate effective tracking and management. To compile such a catalog, several essential steps must be carried out:

1. Correlation: Check if the detected object already exists in the catalog.
2. Orbit Determination: For newly detected objects or updates to existing ones, determine or refine their orbits using sensor data.
3. Catalog Maintenance: Regularly monitor the catalog and schedule new observations as needed.

Once a comprehensive catalog encompassing all detectable Earth-orbiting objects is established and maintained, the following information can be provided:

1. Conjunction Predictions: Providing warnings for potential collisions, known as "conjunction events", between operational spacecraft and space debris.
2. Fragmentation Detection: Identifying when a fragmentation event occurs, whether due to a collision or explosion (e.g., from a discarded rocket stage with remaining fuel or charged batteries), and assessing the evolution of the resulting fragment cloud and associated risks.
3. Reentry Prediction: Calculating the orbital lifetime and determining the reentry date and trajectory of objects.

These tracking capabilities are crucial for managing space debris and ensuring the safety of space operations.

In this thesis, the analysis of fragmentation events relies on publicly available catalogs, acknowledging certain limitations inherent in this approach. Specifically, the study focuses on cataloged events, recognizing that classified objects and undetectable incidents, often attributed to their small size or peculiar orbital characteristics, are excluded from this analysis [4].

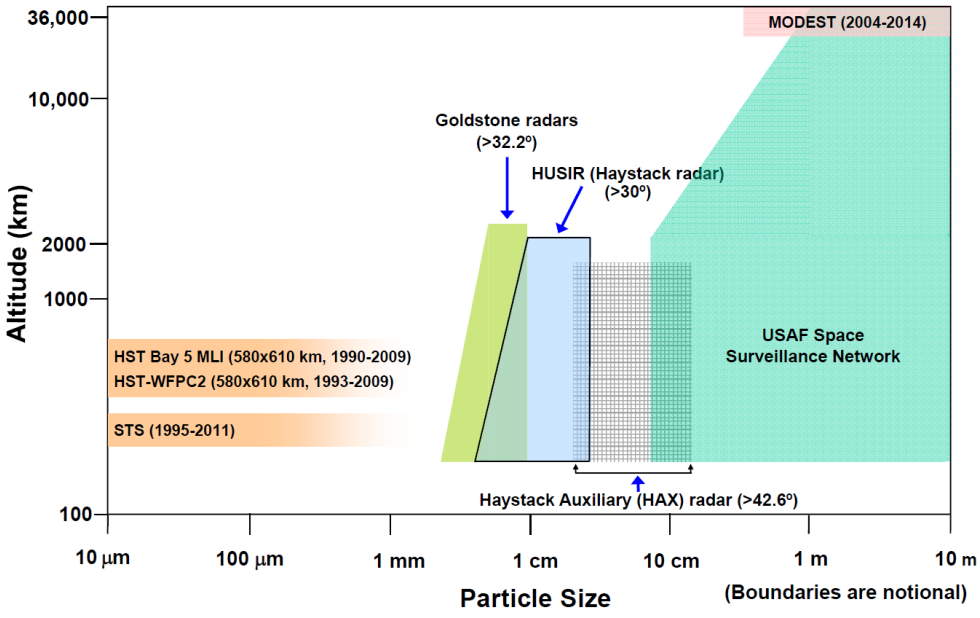

Figure 1.1: U.S. detection capabilities. Credit: NASA ODPO

1.3 Types of space debris

Objects in the space environment can be divided into two main categories: those that can be linked to a specific launch event with identifiable characteristics and those for which this connection is impossible to establish. The latter will be labeled as "Unidentified" (**UI**), while the former can be further classified into:

- Payloads (**PL**): Space objects designed for specific functions in space, excluding launch-related functions. This category encompasses operational satellites as well as calibration objects.

- Payload Mission-Related Objects (**PM**): Space objects intentionally released as space debris that served a purpose in the functioning of a payload. Common examples include protective covers for optical instruments or astronaut tools.

- Payload Fragmentation Debris (**PF**): Space objects that have frag-

mented or were unintentionally released from a payload as space debris, and their origin can be traced back to a specific event. This category includes objects formed during payload explosions or collisions with other objects.

- Payload Debris (**PD**): Space objects that have fragmented or were unintentionally released from a payload as space debris, and while their origin is not entirely clear, their orbital or physical properties allow for a correlation with a source.

- Rocket Bodies (**RB**): Space objects designed to perform launch-related functions. This category includes the various orbital stages of launch vehicles but excludes payloads that release smaller payloads themselves.

- Rocket Mission-Related Objects (**RM**): Space objects intentionally released as space debris that served a purpose for the functioning of a rocket body. Common examples include protective shrouds and engines.

- Rocket Fragmentation Debris (**RF**): Space objects that have fragmented or were unintentionally released from a rocket body as space debris, and their origin can be traced back to a specific event. This category includes objects created during launch vehicle explosions.

- Rocket Debris (**RD**): Space objects that have fragmented or were unintentionally released from a rocket body as space debris, and while their origin is not entirely clear, their orbital or physical properties allow for a correlation with a source.

Every object included in this list becomes a debris when it loses its functionality.

1.4 Fragmentation causes

A fragmentation event can be characterized as an event that generates space debris in space without any specific intended purpose. This includes various

scenarios like collisions, explosions, and natural wear and tear. By adopting this definition of a fragmentation event, it becomes evident how to differentiate between mission-related objects and fragmentation debris.

1.4.1 ESA DISCOS database

The European Space Agency (ESA) Database and Information System Characterising Objects in Space (DISCOS) contains records of space events that have resulted in the creation of additional non-functional objects in Earth's orbit. These events are categorized into main and sub-classes based on their assessed causes. In the first set of classes, the cause of the break-up is well understood:

- **Accidental:** These events resulted from design flaws in subsystems, leading to breakups in some cases. Examples include the breakup of Hitomi (Astro-H) in 2016 and a sub-class related to Oko satellites, such as Cosmos 862 class. The Oko missile early warning satellites carried explosive charges for self-destruction in case of malfunctions, but control of this mechanism was unreliable.
- **Aerodynamics:** Breakups often caused by overpressure due to atmospheric drag.
- **Collision:** Instances where collisions occurred between objects. A subclass includes so-called small impactors, where evidence of an impactor may not be explicit, but changes in angular momentum, attitude, and subsystem failures suggest an impact.
- **Deliberate:** Intentional fragmentation events, including:
  - Anti Satellite Test (ASAT) .
  - Payload recovery failure: Some satellites were designed to explode upon detecting a non-nominal re-entry.
  - Cosmos 2031 class: Orlets reconnaissance satellites introduced in 1989 that employed detonation as a standard procedure after the nominal mission.

  - RORSAT reactor core ejection class: Occurred between 1980 and 1988 when the Soviet Union re-orbited their Radar Ocean Reconnaissance Satellites (RORSAT) and ejected reactor cores, releasing NaK droplets.

- **Electrical:** Most events in this category resulted from overcharging and subsequent battery explosions.

- **Propulsion:** Stored energy in non-passivated propulsion-related subsystems could lead to explosions, e.g., due to thermal stress. Sub-classes relate to rocket stages that experienced repeated breakups, such as Delta upper stage.

A second set of classifications pertains to events with less well-established causes. Events or sub-classes within these categories may be reclassified in the future:

- **Anomalous:** Defined as unplanned separations, usually at low velocity, of one or more objects from a satellite that remains largely intact. This category includes events like debris shedding due to material deterioration, observed from the ground in the past. Sub-classes are defined as events occur multiple times for the same spacecraft or bus type.

  - Transit class: Refers to satellites of the U.S. Navy's first satellite navigation system operational between 1964 and 1996.
  - Scout class: Relates to the Altair upper stage of the Scout rocket family.
  - Meteor class: Pertains to the Russian meteorological satellite family.
  - Vostok class: Refers to the upper stage of the Vostok rocket (Blok E).
  - ERS/SPOT class: Includes ERS-1, ERS-2, and SPOT-4 satellites with confirmed anomalies and catalogued fragments.

  - Delta 4 class: Encompasses events with several catalogued objects for the Delta Cryogenic Second Stages (DCSS).
  - TOPAZ leakage class: For two known events involving TOPAZ satellites, where NaK droplets were observed near the parent object, presumably due to leakage.

- **Assumed:** Introduced for the Meteoroid and Space Debris Terrestrial Environment Reference (MASTER) model, with assumed events primarily in the Geostationary Orbit (GEO) region, supported by information from survey campaigns.

- **Unconfirmed:** A provisional status for events until they are confirmed and classified accordingly.

- **Unknown:** Assigned when there is insufficient evidence to support a more specific classification.

  - Cosmos 699 class: Many ELINT Ocean Reconnaissance Satellites (EORSAT) experienced breakups during orbital decay. Possible causes include deliberate actions, residual propellants, and batteries, but no specific cause was confirmed.
  - L-14B class: The third stage of the Long March 4B (CZ-4B) launcher used hypergolic propellant.
  - H-IIA class: The second stage of the H-IIA launcher used cryogenic propellant.

Applying this classification to all the catalogued fragmentation events as illustrated in Figure 1.2, the predominant category of space incidents involves explosions, particularly those associated with propulsion systems. In contrast, collision events have remained comparatively rare to date. This pattern highlights the past need to comprehensively address and mitigate propulsion-related incidents in space activities. This issue has been successfully addressed over the past two decades, but preventive measures as passivation are still not always applied. In the next sections, fragmentation events have been analyzed in detail.

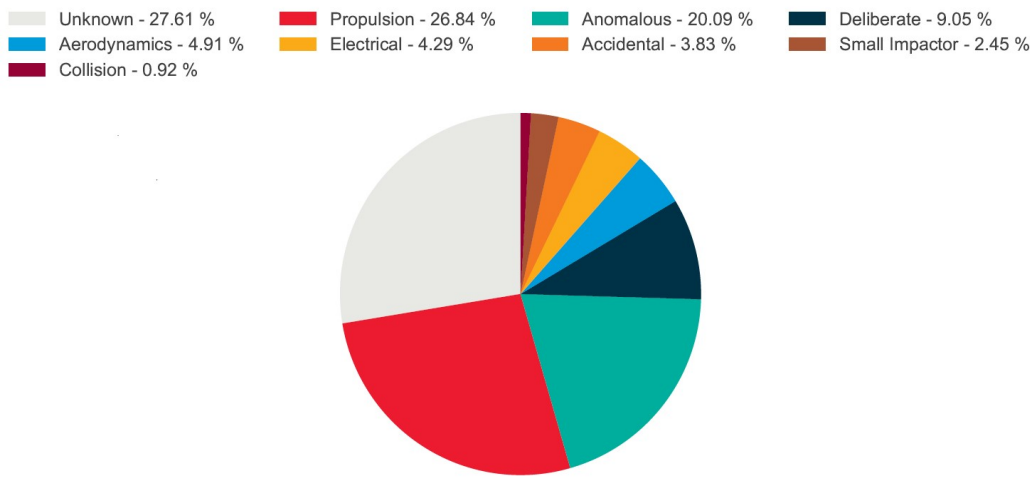

Figure 1.2: Events classification by cause. Credit: ESA

1.5 Space debris, statistics overview

In total, there have been approximately 6420 successful rocket launches, which have placed around 15880 satellites into Earth orbit. Of these satellites, approximately 10590 are still in space, but only about 8600 are currently functioning. In addition to satellites, there are also approximately 34810 pieces of debris that are regularly tracked and catalogued by Space Surveillance Networks. These debris are the result of fragmentation events, such as breakups, explosions, collisions, or other anomalous events. There have been over 640 such fragmentation events since the space age began. The total mass of all space objects in Earth orbit is now over 11000 tonnes [1].

As explained in the previous sections, not all objects are tracked and catalogued. Based on statistical models like ESA MASTER 8, the estimated number of debris objects in orbit as of 2021 is as follows:

- Approximately 36500 space debris objects larger than 10 cm.
- Around 1 million space debris objects ranging from 1 cm to 10 cm in size.
- Roughly 130 million space debris objects measuring from 1 mm to 1 cm.

In Figure 1.3 is shown the growing population of catalogued objects classified by object type, as discussed in Section 1.3. Decayed objects have been excluded from this analysis, and the numbers are constrained by the capabilities of the space surveillance networks available at the time.

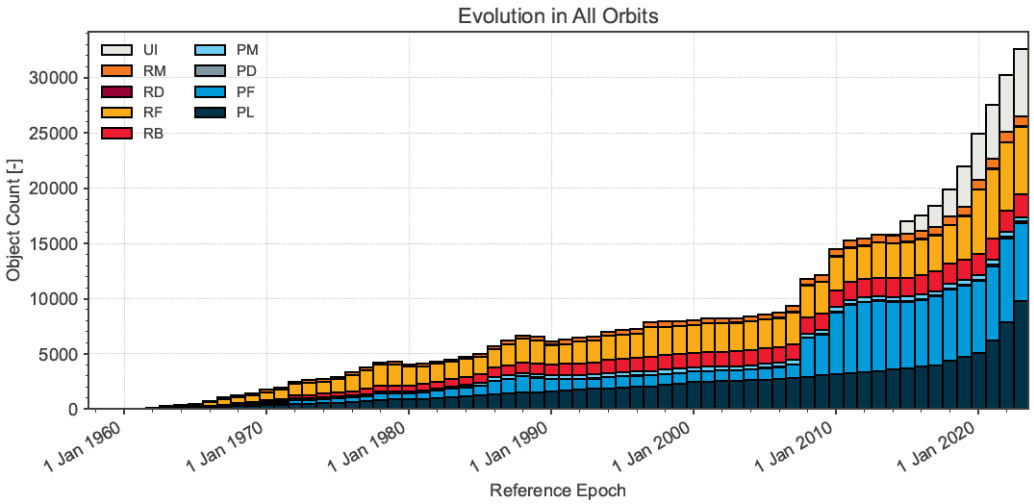

Figure 1.3: Objects in orbit by type over time. Credit: ESA

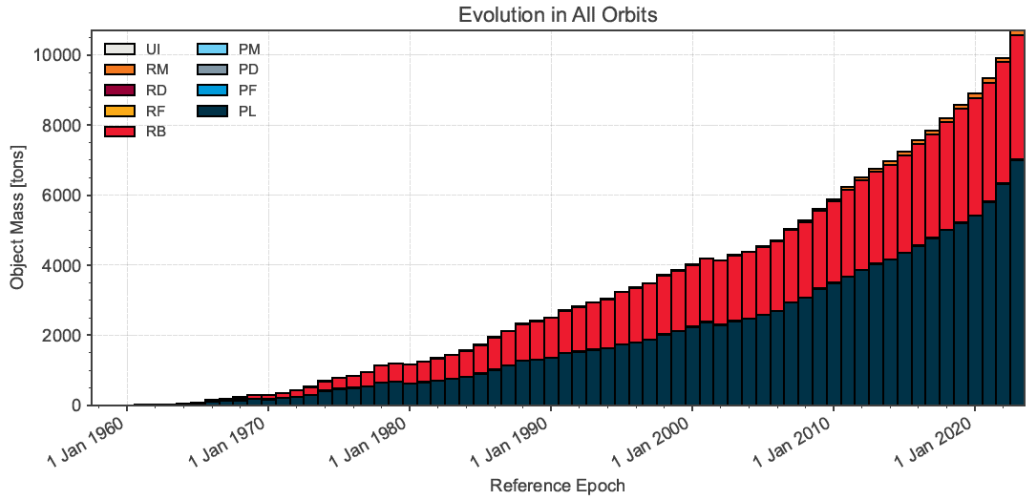

Figure 1.4: Mass in orbit by type over time. Credit: ESA

Over the last decade, there has been a noticeable increase in the number of objects. Figure 1.4 provides insight into the distribution of mass, revealing

that intact objects such as rocket bodies and payloads constitute the majority of the total mass in orbit.

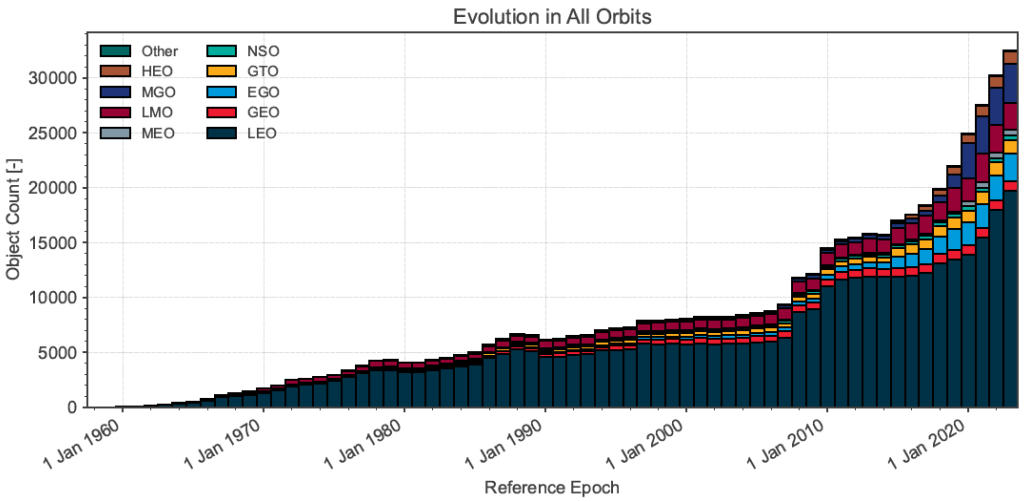

Figure 1.5: Objects by orbit over time. Credit: ESA

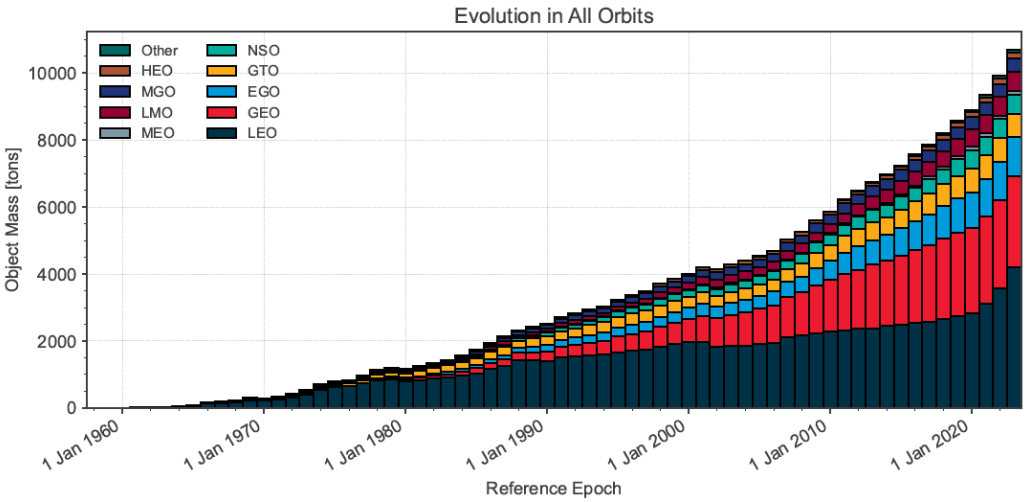

Figure 1.6: Mass by orbit over time. Credit: ESA

Figure 1.5 categorizes objects in orbit by their orbit type (described in Table 1.1), highlighting a higher population density in LEO. Additionally, upon comparing Figure 1.5 and Figure 1.6, it has been observed that objects launched in LEO tend to be lighter compared to those in other orbits.

Orbit	Orbit Description	Definition		
GEO	Geostationary	$i \in [0, 25]$	$hp \in [35586, 35986]$	$ha \in [35586, 35986]$
IGO	Inclined Geosynchronous	$a \in [37948, 46380]$	$e \in [0.00, 0.25]$	$i \in [25, 180]$
EGO	Extended Geostationary	$a \in [37948, 46380]$	$e \in [0.00, 0.25]$	$i \in [0, 25]$
NSO	Navigation Satellites	$i \in [50, 70]$	$hp \in [18100, 24300]$	$ha \in [18100, 24300]$
GTO	GEO Transfer	$i \in [0, 90]$	$hp \in [0, 2000]$	$ha \in [31570, 40002]$
MEO	Medium Earth	$hp \in [2000, 31570]$	$ha \in [2000, 31570]$	
GHO	GEO-superGEO Crossing	$hp \in [31570, 40002]$	$ha > 40002$	
LEO	Low Earth	$hp \in [0, 2000]$	$ha \in [0, 2000]$	
HAO	High Altitude Earth	$hp > 40002$	$ha > 40002$	
MGO	MEO-GEO Crossing	$hp \in [2000, 31570]$	$ha \in [31570, 40002]$	
HEO	Highly Eccentric Earth	$hp \in [0, 31570]$	$ha > 40002$	
LMO	LEO-MEO Crossing	$hp \in [0, 2000]$	$ha \in [2000, 31570]$	
UFO	Undefined			
ESO	Escape			

Table 1.1: Orbit classification. Credit: ESA

1.5.1 Fragmentation events

In the previous section, it was mentioned that propulsion-related incidents, such as explosions, have been the most common cause of fragmentation among those that have been identified. However, when we compare Figure 1.7 and Figure 1.8, it can be noticed that deliberate events have generated a larger number of fragments, despite occurring less frequently.

Anomalous events, as defined previously, are characterized by a relatively small number of fragments.

Regarding aerodynamic events, the number of fragments is relatively low because they typically occur at lower altitudes. This exposes the produced fragments to atmospheric drag, leading to their relatively rapid reentry into the Earth's atmosphere. In some cases, these fragments may reenter so swiftly that they cannot even be catalogued in time.

The peak in fragments produced between 2005-2010 can be attributed to the ASAT test on Fengyun-1C in 2007 and the accidental hypervelocity collision involving Iridium 33 and Cosmos 2251 in 2009. These events are among the most severe catalogued fragmentations in history.

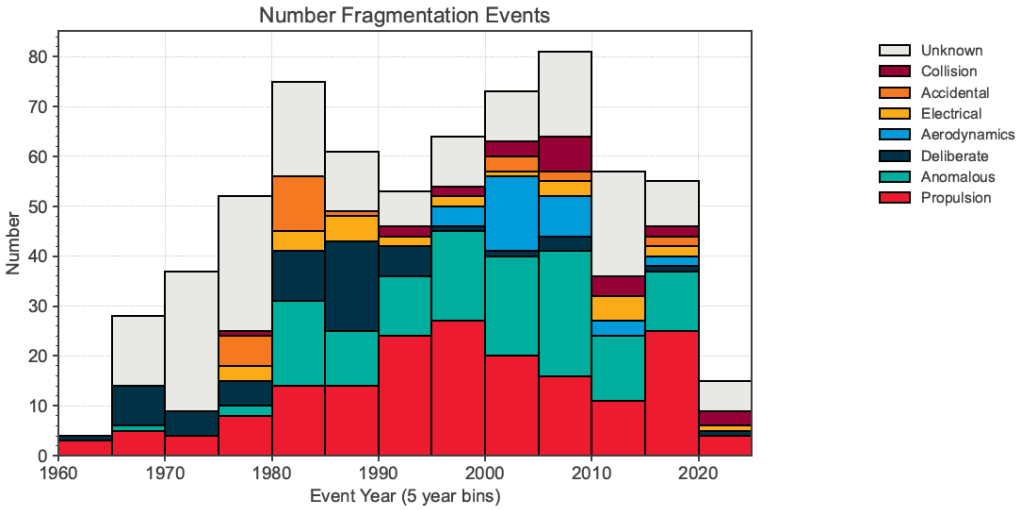

Figure 1.7: Events by cause per year. Credit: ESA

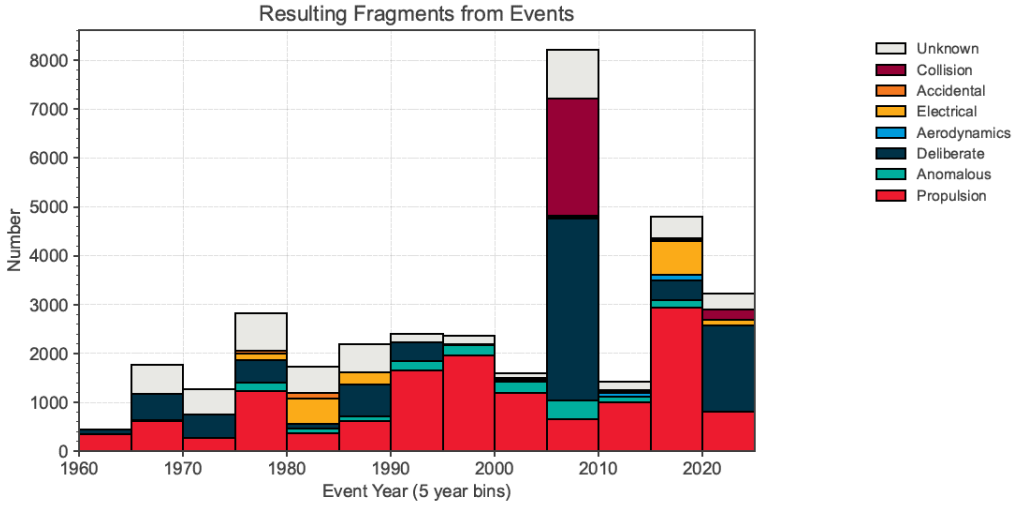

Figure 1.8: Fragments by cause per year. Credit: ESA

1.6 Thesis scope

This thesis delves into the phenomenon of in-orbit catastrophic fragmentations, conducting a comprehensive analysis of existing models and providing a definition of "catastrophic breakup" based on observed historical data. It also explores failure modes that could be included in the given definition, with a specific focus on their impact on the space debris environment. Following

this, a case study is carried out to assess the probability of a catastrophic breakup occurring under the defined thresholds, while also examining potential mitigation strategies.

Chapter 2

Catastrophic fragmentations

There is no universally accepted definition of catastrophic fragmentation in the literature; however, a distinction based on common sense can be made. A fragmentation event can be considered catastrophic in the following ways:

- For the mission: A fragmentation event damages at least one critical component for achieving the mission objectives to a degree that compromises the mission's success. This includes scenarios where vital mission instruments or systems are rendered inoperable due to the event.
- For specific spacecraft functionalities:
  - Communication capabilities: A fragmentation event that leads to the loss of communication with the spacecraft. In such cases, the spacecraft may become unresponsive, hindering data transmission and control.
  - Post Mission Disposal (PMD) capabilities: A fragmentation event that results in the loss of PMD capabilities. PMD involves safely deorbiting or relocating a spacecraft at the end of its operational life to prevent space debris generation. Losing this capability can have long-term implications for space sustainability.
- For the structural integrity of the spacecraft: A fragmentation event

that causes significant damage to the spacecraft. This damage can include physical harm to the spacecraft's structure, making it less functional or posing risks to its stability.

- For the environment: The fragmentation event generates additional hazards in the space environment. This can include the creation of numerous debris fragments that pose collision risks to operational satellites and other objects in orbit, potentially increasing the space debris problem.

It's important to note that the first category, related to the mission success, is highly subjective and depend on the specific mission and spacecraft. Therefore, these subjective criteria have not been considered in this study, which focuses on more objective factors related to fragmentation events.

As tracking capabilities are limited and for mitigation purposes, it's crucial to develop models that can estimate the outcomes of in-space fragmentations.

2.1 NASA Standard Breakup Model

The NASA Standard Breakup Model (SBM) describes the outcome of a satellite breakup and provides: the number of fragments, their Area-to-Mass ratio (A/m), and the velocity distributions. Velocity distribution is not handled in this thesis [5][6].

NASA SBM defines the catastrophic and non-catastrophic collisions focusing on the structural integrity of the objects, and it consider the two main fragmentation events: explosion and collision. The development of the SBM, was reliant on data gathered since the early 1980s. This data included:

1. Deliberate hypervelocity collisions in LEO in 1985 and 1986, involving the Solwind (P-78) and the USA 19 (Delta-180) missions, respectively.

2. The Satellite Orbital Debris Characterization Impact Test (SOCIT) series conducted on the ground in 1991 and 1992.

3. Sub-scale explosion tests of Ariane upper stages overseen by the ESA.

4. A comprehensive compilation of historical orbital data, specifically two-line element sets, which were utilized to determine ejection velocity and A/m distributions.

2.1.1 Characteristic length

The model used in EVOLVE 4.0, the software implementing the NASA SBM, consider the characteristic length as free parameter instead of the mass, as in the previous implementations. This allows radar observations to be utilized for deriving the characteristic length, denoted as L_c, from the radar cross-section (RCS). Assuming the body is spherical, the characteristic length (diameter) L_c can be calculated from the radar cross-section, which is considered as a two-dimensional circular area:

$$L_c = 2\sqrt{\frac{RCS}{\pi}} \tag{2.1}$$

Another method for determining the characteristic length L_c involves averaging the three maximum orthogonal dimensions:

$$L_c = \frac{1}{3} \cdot (X + Y + Z) \tag{2.2}$$

While L_c serves as the independent variable, the relation between size and mass of the fragments can be useful to evaluate the Energy-to-Mass Ratio (EMR). Assuming the object as spherical:

$$\rho(L_c) = \begin{cases} 2698.9 & \text{if } L_c < 0.01m \\ 92.937 \cdot Lc^{-0.74} & \text{if } L_c \geq 0.01m \end{cases} \tag{2.3}$$

$$m(L_c) = \frac{4}{3}\pi \left(\frac{L_c}{2}\right)^3 \cdot \rho(L_c) \tag{2.4}$$

Here, ρ represents density in kg/m^3, L_c is in meters, m is in kilograms.

2.1.2 NASA SBM for explosions

The empirical model is based on the fragment distribution of 7 observed on-orbit rocket booster (R/B) explosions:

- Fragments are described by a single power law distribution.
- Explosions are classified into 6 different groups with different unitless scaling factors (s) assigned to their fragment distribution, as shown in Table 2.1. The scaling factor is between 0 and 1, where it is equal to 1 for rocket boosters with a mass of 600 to 1000 kg.

The cumulative number of fragments (N) greater than or equal to the L_c is given by the equation:

$$N(L_c) = s \cdot 6 \cdot L_c^{-1.6} \tag{2.5}$$

Where N is the number of fragments greater than or equal to L_c, L_c is the characteristic length in meters.

Event Type	s
SL-12 ullage motor	0.1
Cosmos 699 class	0.6
Cosmos 862 class	0.1
All Soviet/Russian battery-related events	0.5
All Soviet/Russian ASAT	0.3
Other satellites / rocket bodies	1.0

Table 2.1: Scaling factor by event type

2.1.3 NASA SBM for collisions

In this case the distinction between a catastrophic and non-catastrophic collision hinges on the EMR. For collisions, the input parameters consist of the masses of the two colliding space objects (referred to as parents) and the impact velocity. According to the SBM, collisions can be categorized as either catastrophic, where both parent objects are fully fragmented, or

non-catastrophic, where the projectile fragments and the target experiences cratering. The distinction between catastrophic and non-catastrophic collisions is determined by evaluating the relative kinetic energy of the projectile divided by the mass of the target (EMR). Specifically, a collision is classified as catastrophic if the value of EMR exceeds 40 J/g.

$$EMR = \frac{1}{2} m_{projectile} \Delta v^2 / m_{target} \tag{2.6}$$

Here, $m_{projectile}$ is in kilograms and m_{target} is in grams, while Δv represents the relative impact velocity in m/s.

The cumulative number of fragments for collision is calculated as:

$$N(L_c) = 0.1 \cdot M^{0.75} \cdot L_c^{-1.71} \tag{2.7}$$

Where:

$$M = \begin{cases} m_{target} + m_{projectile} & \text{if catastrophic} \\ m_{projectile} \cdot \Delta v^2 & \text{if non-catastrophic} \end{cases} \tag{2.8}$$

Here both masses are expressed in kilograms and Δv in km/s.

2.1.4 Area-to-mass distributions

Aside from L_c, the A/m is the second parameter generated by the NASA SBM. Therefore, the simulation has to draw values from which both rely on the normal distribution. Further, the A/m distribution does not distinguish between the two types, explosion and collision.

In general, these ratios serve as a reasonably accurate approximation of the actual average A/m. However, when the calculated A/m reaches large values ($> 1\ m^2/kg$), the influence of solar radiation pressure becomes significant. As a result, for such objects, the calculated A/m is more effective for determining orbital lifetime than for establishing debris mass through a relationship with L_c.

For debris with a $L_c > 11\ cm$, A/m distributions have been established by

examining the decay rates of cataloged debris. The A/m for fragments larger than 11 cm is estimated as:

$$\begin{aligned} D_{A/m}(\lambda_c, \chi) =& \alpha(\lambda_c) \cdot N(\mu_1(\lambda_c), \sigma_1(\lambda_c), \chi) + \\ &+ (1 - \alpha(\lambda_c)) \cdot N(\mu_2(\lambda_c), \sigma_2(\lambda_c), \chi) \end{aligned} \tag{2.9}$$

Where:

- $\lambda_c = \log_{10}(L_c)$
- $\chi = \log_{10}(A/m)$ is the variable in the distribution
- N is the normal distribution function:

$$N(\mu, \sigma, \chi) = \frac{1}{\sigma\sqrt{2\pi}} \cdot \exp\left(-\frac{(\chi - \mu)^2}{2\sigma^2}\right) \tag{2.10}$$

The equations use different parameters if the debris are generated from a rocket booster (R/B) or a spacecraft (S/C). Parameters for the A/m distribution for rocket booster fragments (R/B) and greater than 11 cm:

$$\begin{aligned} \alpha^{R/B} &= \begin{cases} 1 & \lambda_c \leq -1.4 \\ 1 - 0.3571(\lambda_c + 1.4) & 1.4 < \lambda_c < 0 \\ 0.5 & \lambda_c \geq 0 \end{cases} \\ \mu_1^{R/B} &= \begin{cases} -0.45 & \lambda_c \leq -0.5 \\ -0.45 - 0.9(\lambda_c + 0.5) & -0.5 < \lambda_c < 0 \\ -0.9 & \lambda_c \geq 0 \end{cases} \\ \sigma_1^{R/B} &= 0.55 \\ \mu_2^{R/B} &= -0.9 \\ \sigma_2^{R/B} &= \begin{cases} 0.28 & \lambda_c \leq -1.0 \\ 0.28 - 0.1636(\lambda_c + 1) & -1.0 < \lambda_c < 0.1 \\ 0.1 & \lambda_c \geq 0.1 \end{cases} \end{aligned} \tag{2.11}$$

Parameters for the A/m distribution for S/C fragments greater than 11 *cm*:

$$
\begin{aligned}
\alpha^{S/C} &= \begin{cases} 0 & \lambda_c \leq -1.95 \\ 0.3 + 0.4\,(\lambda_c + 1.2) & -1.95 < \lambda_c < 0.55 \\ 1 & \lambda_c \geq 0.55 \end{cases} \\
\mu_1^{S/C} &= \begin{cases} -0.6 & \lambda_c \leq -1.1 \\ -0.6 - 0.318\,(\lambda_c + 1.1) & -1.1 < \lambda_c < 0 \\ -0.95 & \lambda_c \geq 0 \end{cases} \\
\sigma_1^{S/C} &= \begin{cases} 0.1 & \lambda_c \leq -1.3 \\ 0.1 + 0.2\,(\lambda_c + 1.3) & -1.3 < \lambda_c < -0.3 \\ 0.3 & \lambda_c \geq -0.3 \end{cases} \\
\mu_2^{S/C} &= \begin{cases} -1.2 & \lambda_c \leq -0.7 \\ -1.2 - 1.333\,(\lambda_c + 0.7) & -0.7 < \lambda_c < -0.1 \\ -2.0 & \lambda_c \geq -0.1 \end{cases} \\
\sigma_2^{S/C} &= \begin{cases} 0.5 & \lambda_c \leq -0.5 \\ 0.5 - (\lambda_c + 0.5) & -0.5 < \lambda_c < -0.3 \\ 0.3 & \lambda_c \geq -0.3 \end{cases}
\end{aligned}
\tag{2.12}
$$

The Equation (2.13) calculates the A/m values for debris smaller than 8 *cm*. Unlike the former Equation (2.9), it does not distinguish between the origin of the fragments, and therefore, it has a unique parameter set (Equation (2.14)). The abbreviation SOC used here is based on the experimental series SOCIT, as mentioned earlier.

$$
D_{A/m}^{SOC}(\lambda_c, \chi) = N(\mu^{SOC}(\lambda_c), \sigma^{SOC}(\lambda_c), \chi) \tag{2.13}
$$

Parameters for the A/m distribution for fragments smaller than 8 *cm*:

$$\mu^{SOC} = \begin{cases} -0.3 & \lambda_c \leq -1.75 \\ -0.3 - 1.4\,(\lambda_c + 1.75) & -1.75 < \lambda_c < -1.25 \\ -1.0 & \lambda_c \geq -1.25 \end{cases} \tag{2.14}$$

$$\sigma^{SOC} = \begin{cases} 0.2 & \lambda_c \leq -3.5 \\ 0.2 + 0.1333\,(\lambda_c + 3.5) & \lambda_c > -3.5 \end{cases}$$

A bridge function is used for fragments between 8 cm and 11 cm.

2.2 Considerations on the EMR threshold

As previously mentioned, the SBM primarily focuses on assessing the structural integrity of space objects involved in fragmentation events. Over the years, the model has undergone extensive testing. It may tend to overestimate small fragments with L_c under 1 cm, but for $L_c = 10$ cm, the model provides an acceptable estimation within the scope of this thesis. It relies on the EMR as a key parameter for estimating the number of fragments produced during such events. However, it's important to note that the outcome of a fragmentation event is not determined only by the EMR; there are other influential factors to consider.

One critical aspect that the model does not account for is the specific point of impact during a collision event. For example, in a glancing impact, the calculated EMR may exceed 40 J/g, as defined by the model for catastrophic collisions. However, this elevated EMR value does not guarantee complete fragmentation of the parent objects [7]. The angle and location of impact are critical determinants of the outcome, which can lead to an overestimation of the number of fragments produced. Consequently, the critical section for catastrophic collisions may be considerably smaller than the actual cross-section.

Remarkably, the majority of the published long-term evolutionary analyses, including those that compare various models, have not explicitly addressed

the incorporation of specific cross-section reduction factors for collision modeling [8].

Additionally, the geometry of the target object is another essential factor that can significantly influence the production of fragments. For instance, a spacecraft with interconnected modules or appendices may experience a partial fragmentation of one of these components during a collision. This partial fragmentation can still generate a substantial number of fragments, even though other parts of the spacecraft remain structurally intact [9]. This might represent a unique case that has not been documented previously.

In summary, while EMR is a valuable parameter in the SBM for categorizing catastrophic and non-catastrophic collisions, it is essential to consider the broader context, including the point of impact and target geometry, to accurately assess the outcome of fragmentation events. These additional factors can impact the number and distribution of fragments generated during space collisions.

2.3 Evolutionary models

NASA LEO-to-GEO Environment Debris Model (LEGEND) is a three-dimensional numerical simulation model for long-term studies of orbital debris evolution. It has replaced the one-dimensional model EVOLVE, which was limited to LEO. These models have the capability to predict future debris environments based on user-specified scenarios but are significantly influenced by the underlying breakup model. The latest version of MASTER 8 also utilizes NASA SBM to estimate future debris spatial densities and fluxes, as detailed in [10].

The SBM has been used in all long-term projections of the LEO debris population, specifically for estimating the number of explosion and collision fragments for objects with $L_c > 10\ cm$.

In this projection, it was assumed that future launch traffic could be represented by the repetition of the 2001 to 2009 traffic cycle. Then, the commonly

adopted mitigation measures were assumed to be well-implemented. In particular, a compliance of 90% with the PMD 25-year rule for spacecrafts and upper stages and a 100% success for passivation (no future explosions) were assumed. Collision avoidance maneuvers were not allowed.

Results showed the LEO debris populations are projected to grow by an average of 30% over the next 200 years. This growth is predominantly influenced by catastrophic collisions occurring at altitudes between 700 and 1000 km, with such collisions expected to take place approximately every 5 to 9 years [11].

NASA LEGEND projection results of the non-mitigation scenario and PMD and Active Debris Removal (ADR) are shown in Figure 2.1 and Figure 2.2. It's important to note that these simulations were performed over a decade ago.

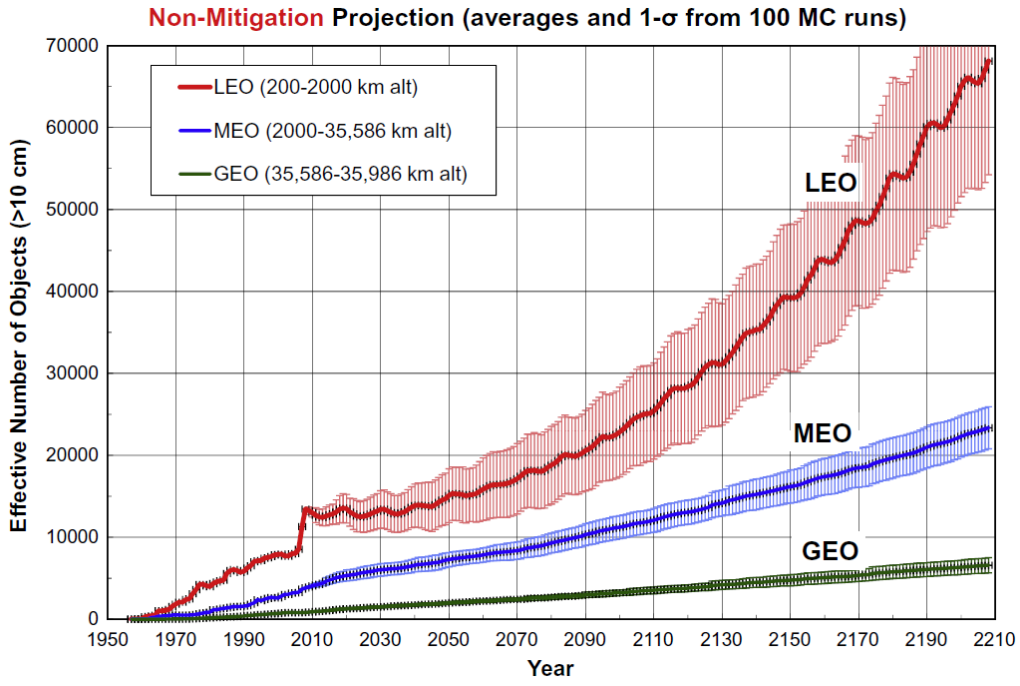

Figure 2.1: LEGEND projection, no mitigation scenario [12]

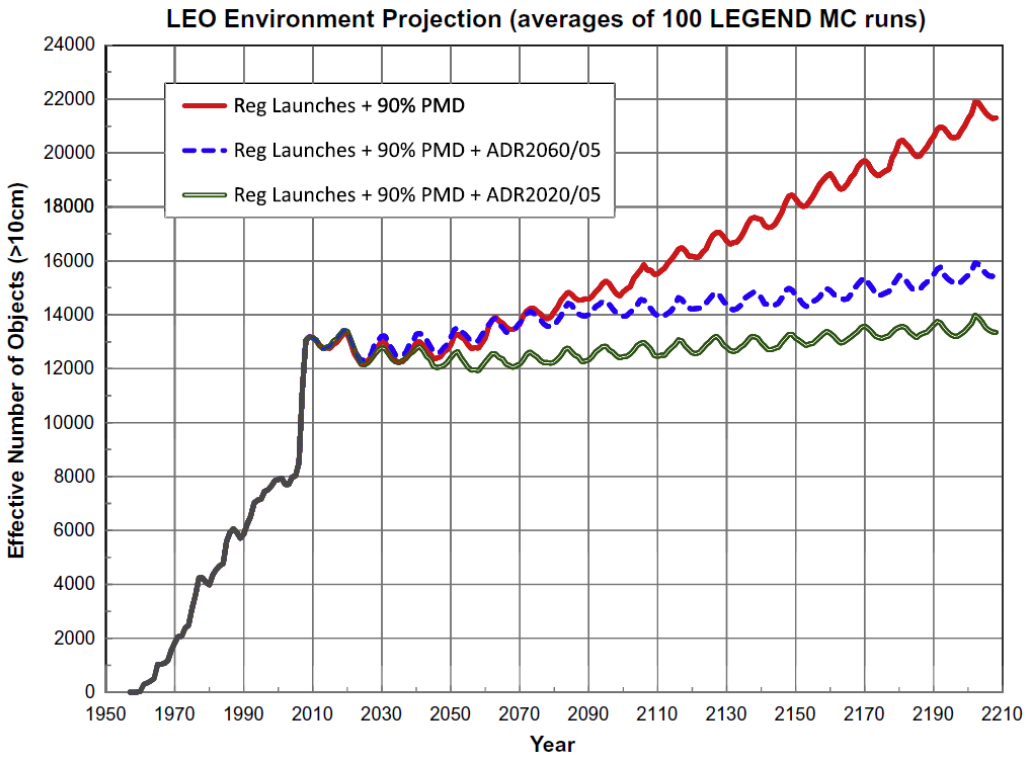

Figure 2.2: LEGEND projection, PMD and ADR scenario [12]

Chapter 3

Catastrophic for the environment

In this chapter, a new perspective on the definition of catastrophic fragmentation is introduced, which shifts away from the previous emphasis on the structural integrity of the spacecraft. In the context of space debris management and the preservation of orbital environments, it becomes essential to distinguish between different types of fragmentation events and their potential impact. This distinction enables the determination of when a fragmentation event can be classified as catastrophic and, as a result, deserving special attention.

1. **Catastrophic breakup:** This category encompasses events that result in the generation of a significant number of both small and large fragments. These fragments can have a substantial and lasting impact on both the short-term and long-term orbital environment, posing a significant challenge for space debris mitigation efforts.

2. **Non-catastrophic breakup:** In contrast, non-catastrophic breakup events produce a population of smaller fragments. While these events may not have as profound a long-term impact as catastrophic ones, they can still affect the short-term orbital environment and require consideration in space debris management strategies.

3. **Minor breakup:** Lastly, minor breakup events are those that have a negligible effect on the overall orbital environment. These events may

result in limited or no fragmentation, and their impact on space debris conditions is minimal.

This classification system helps in understanding the severity of fragmentation events and guides decisions related to space debris mitigation and prevention.

3.1 Definitions and threshold values

When selecting parameters for assessing catastrophic fragmentation, it is essential to ensure they align with the previously defined criteria while also being straightforward to evaluate. Key parameters to consider include:

- Production of a specific number of fragments of a particular size.
- Mass fragmented, which also encompasses large derelicts that remain uncontrolled.
- In-orbit persistence, measured on a per-object basis.

The choice of parameter values should be made with careful consideration of their potential consequences on the orbital environment.

In the subsequent paragraphs, the threshold values for each category are documented. The rationale behind these choices is extensively discussed in the following subsections.

Catastrophic breakup

With the previous considerations in mind catastrophic breakup is defined as follows:

- More than 100 catalogued debris objects with a characteristic length (L_c) greater than 10 cm.
- More than 100 kg of fragmented mass produced as a result of the event.

- More than 50 of these debris objects are expected to persist in orbit for at least 25 years.

This definition provides specific criteria for identifying catastrophic breakup events based on the number of debris objects, their size, fragmented mass, and orbital persistence.

Non-Catastrophic breakup

Following the same path, non-catastrophic breakup is defined as:

- More than 10 catalogued debris objects with a characteristic length (L_c) greater than 10 cm.
- More than 10 kg of fragmented mass produced as a result of the event.
- More than 5 of these debris objects are expected to persist in orbit for at least 5 years.

This definition provides specific criteria for identifying non-catastrophic breakup events based on the number of debris objects, their size, fragmented mass, and orbital persistence. Non-catastrophic breakup events have to result in a smaller number of debris objects with shorter orbital lifespans compared to catastrophic breakup events.

Minor breakup

So minor breakup events are defined as:

- Less than 10 catalogued debris objects with a characteristic length (L_c) greater than 10 cm.
- Less than 10 kg of fragmented mass produced as a result of the event.
- Less than 5 of these debris objects are expected to persist in orbit for at least 5 years.

By establishing these clear definitions and criteria, it becomes possible to categorize and evaluate fragmentation events based on their potential consequences.

3.1.1 Debris production

The rationale behind setting the size threshold at $L_c > 10\ cm$ has multiple reasons. Firstly, it is grounded in the recognition that debris of this size possesses the potential to initiate a subsequent catastrophic collision. This potential consequence is assessed through the EMR calculation, considering the average collision velocity in LEO of 10 km/s. For the purposes of this determination, are considered two different cases:

1. The first case assumes the debris to be spherical and composed of aluminum without accounting for the diminishing density concept as described in Equation (2.3). This leads to a catastrophic EMR.

2. The second one uses the diminishing density concept for calculating the mass of a 10 cm debris. This would lead to a catastrophic EMR for small satellites ($< 500\ kg$ of mass). For an impact with a larger satellite (e.g. 1000 kg of mass), the EMR doesn't reach the catastrophic threshold, but it will generate enough (more than a hundred) large debris to be classified as a catastrophic breakup. So the collision will be non-catastrophic for the NASA SBM but it will be a catastrophic breakup for the space debris environment.

Both cases can generate a large number of fragments that can cause a subsequent catastrophic breakup.

Furthermore, this chosen size threshold is in harmony with the tracking capabilities of catalogued objects in LEO, establishing a practical benchmark for differentiation. Catalogued objects are those with observational data supporting their existence rather than relying only on theoretical models. This alignment in size criteria enhances the likelihood that objects surpassing this threshold can be effectively monitored and tracked within the orbital environment, enhancing their reliability.

Examining historical fragmentation data [13] [14] [15] and classifying them based on the number of cataloged fragments (N) yields several significant

findings. Figure 3.1 presents a visual representation of these events categorized by the quantity of generated objects, while Figure 3.2 provides a graphical representation of the cumulative fragments generated within the corresponding classifications.

It becomes evident that a significant portion of fragmentation events, approximately 49% (as demonstrated in Figure 3.1), resulted in the production of only about 3% of the catalogued debris (as indicated in Figure 3.2). These events typically involve ten or fewer catalogued debris objects. Conversely, a relatively small percentage of fragmentation events, roughly 1%, generated over 28% of the entire debris catalog. These events are characterized by the production of more than a thousand catalogued debris objects.

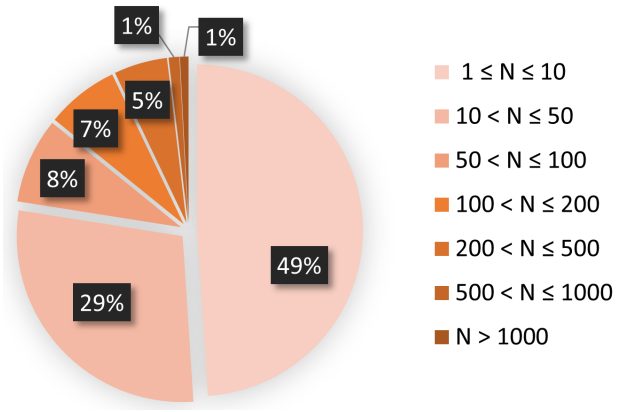

Figure 3.1: Events classification by fragment production

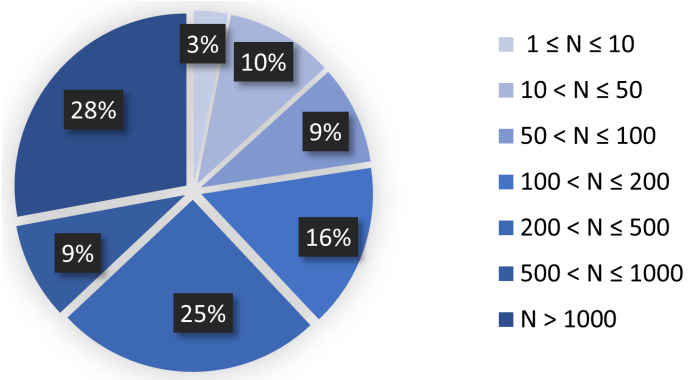

Figure 3.2: Cumulative fragments production by event

The definitions from Section 3.1 have been applied to the classifications previously presented in Figure 3.1 and Figure 3.2, resulting in the updated visualizations shown in Figure 3.3 and Figure 3.4.

Among the considered threshold values, the 100 debris fragments with $L_c > 10\ cm$ stand out as critical parameters for assessing the space environment. This threshold is associated with approximately 78% of the total fragments, generated by just around 14% of the events.

Altering this threshold could lead to a misrepresentation of the space debris environment. For instance, reducing the catastrophic threshold to include events with fewer debris fragments may introduce numerous events of lesser significance, making it challenging to compare them with more substantial events. For example, if the threshold is set at 50 debris produced, approximately 22% of the events produce around 86% of the fragments, and these additional events generate fragments that are an order of magnitude fewer than the major events. Conversely, raising the threshold to a higher value, such as 200 produced fragments, results in approximately 7% of the events generating about 62% of the fragment population.

Applying these insights this simple classification demonstrates that a threshold value of 100 debris with $L_c > 10\ cm$ plays a critical role in the space environment.

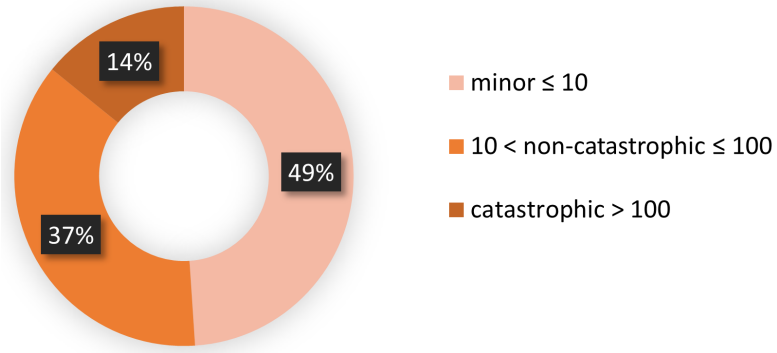

Figure 3.3: Events classification by fragment production, updated definition

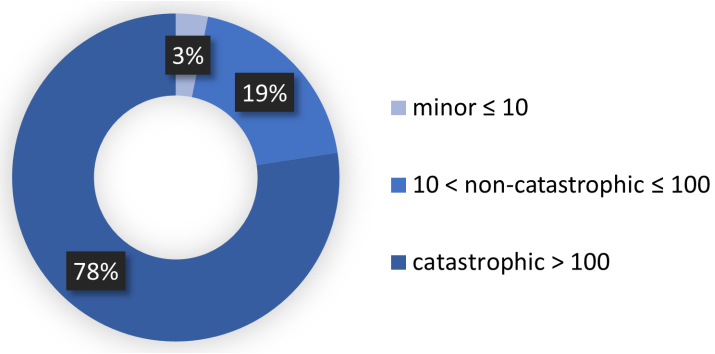

Figure 3.4: Cumulative fragments production by event, updated definition

3.1.2 Fragmented mass

The fragmented mass usually is not known and it has to be modeled starting from the number of fragments using NASA SBM or estimated starting from ground observations [16] [17].

To model the fragmented mass the NASA SBM propose to evaluate the cross sectional area (A_x) of the fragments as:

$$A_x(L_c) = \begin{cases} 0.540424 \cdot L_c^2 & L_c < 0.00167m \\ 0.556945 \cdot L_c^{2.0047077} & L_c \geq 0.00167m \end{cases} \tag{3.1}$$

Then the mass is given by:

$$M = \frac{A_x}{A/m} \tag{3.2}$$

Where the A/m distribution can be calculated as shown in Section 2.1.4.

Alternatively, an alternative approach relies on ground-based observations of the fragments. In this method, the A/m ratio is derived from the orbital decay of objects. The cross-sectional areas and fragment masses are computed using the same equations as detailed in Equation (3.1) and Equation (3.2).

The threshold value of 100 kg of fragmented mass, chosen in Section 3.1, reflects the debris production threshold as a 100 kg complete fragmented object can generate up to $\sim$ 160 debris with $L_c > 10$ cm, according to the

NASA SBM. Applying the same criteria to the non-catastrophic breakup mass threshold, 10 kg will produce $\sim$ 30 debris. Both mass thresholds result coherent with the debris production thresholds.

3.1.3 Debris lifetime

Estimating the lifetimes of debris clouds is a complex task due to the multitude of variables influencing orbital decay. Key factors include the A/m ratio, which affects atmospheric drag, and the cross-section, which plays a crucial role in evaluating the impact of solar radiation pressure.

One approach to estimate lifetimes involves observing the orbital decay of objects and calculating the ballistic coefficient, which can also be found in the public Two Line Element set (TLE) available on Space-Track. Subsequently, lifetimes can be determined using orbital propagators. However, it's essential to bear in mind that most orbital propagators typically do not account for solar radiation pressure.

In simple terms, objects with a perigee altitude greater than 600 km are expected to remain in orbit for way more than 25 years. This extended orbital lifetime also means that they will eventually enter the densely populated LEO region, typically between 700 and 1000 km in altitude. This poses a long-term space debris hazard for this region [18].

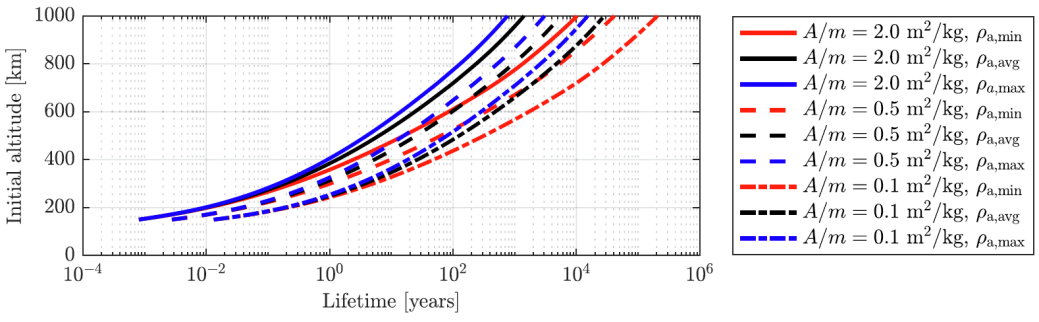

Figure 3.5: Expected lifetime of space debris by A/m [19]

Figure 3.5 provides lifetime estimates for large objects ($L_c > 10$ cm) with

different A/m and atmospheric densities (ρ_a). Minimum ($\rho_{a,min}$) and maximum ($\rho_{a,max}$) atmospheric density values depend on the solar activity level for altitudes between 120 and 2000 km [20], while $\rho_{a,avg} = (\rho_{a,min} + \rho_{a,max})/2$.

This method neglects the significant impact of solar radiation pressure, which can notably reduce the expected lifetime of the objects. Further validation through simulations is necessary for this aspect. Specific cases related to the calculations of lifetime values will be examined in the following sections.

3.2 Catalogued breakups

In this section, we analyze several breakup events, with a particular focus on collisions, and how they affect the space debris environment [13] [14] [15].

3.2.1 Catastrophic breakup events

These events are included in the catastrophic breakup definition, generating a substantial population of large fragments that will affect the long term space debris environment.

Fengyun-1C ASAT

The deliberate breakup of Fengyun-1C on January 11, 2007, resulted in the formation of the most severe orbital debris cloud in history. This 880 kg defunct meteorological satellite was orbiting in a polar orbit at an altitude of 860 km when it collided with a kinetic kill vehicle estimated to have a mass of about 600 kg [21].

The impact occurred at a velocity of approximately 9.4 km/s, generating 3521 cataloged fragments larger than 10 cm, with 2854 still in orbit. Notably, over half of the identified debris fragments were thrown into orbits exceeding an average altitude of 850 km. As a result, a substantial portion of the debris, measuring 10 cm or larger, is expected to remain in orbit for decades or even centuries.

A notable aspect of the Fengyun fragment distribution is the prevalence of fragments with a high A/m, measuring 0.1 m^2/kg and above. This can be attributed to the presence of two sizable solar panels, each measuring 1.5 m by 4 m, and approximately 13 m^2 of Multi Layer Insulation (MLI) on the spacecraft's surface. It is highly probable that the high A/m component of these fragments comprises, at least to some extent, pieces from the solar panels and MLI. Additionally, lightweight plastic materials may also contribute to the high A/m distribution.

This fact pointed out the discrepancy between the A/m distribution observed and the one modeled through the NASA SBM, which have significantly underestimated the A/m of the fragments [22]. One possible explanation for this discrepancy could be that the model is ill-suited to account for the characteristics of newer lightweight materials.

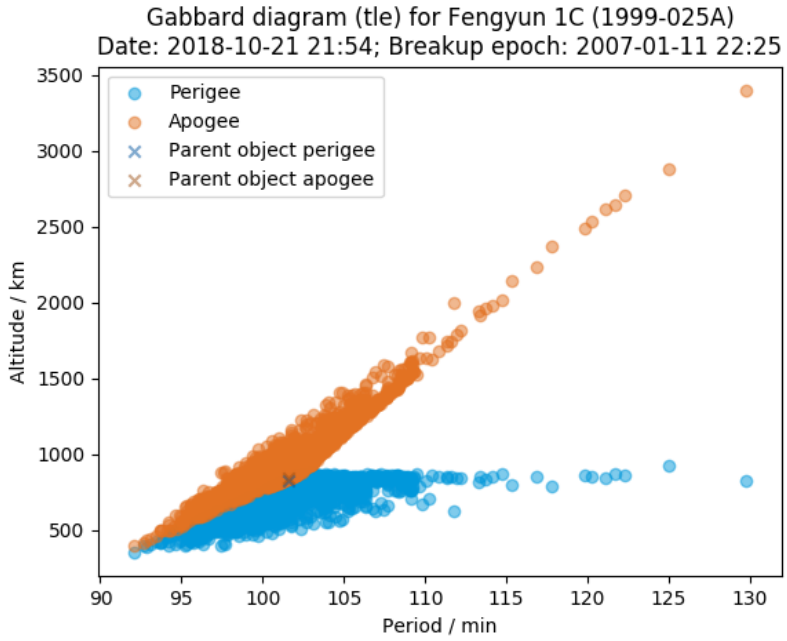

Figure 3.6: Gabbard diagram of Fengyun 1C fragments. Credit: ESA

Figure 3.6 illustrates the distribution of fragments from Fengyun 1C ASAT on the Gabbard diagram 11 years after the event. Meanwhile, Figure 3.7 and Figure 3.8 depict the increase in risk by altitude resulting from the

event. This risk is evaluated with respect to the MASTER 2009 population, assuming a business-as-usual projection.

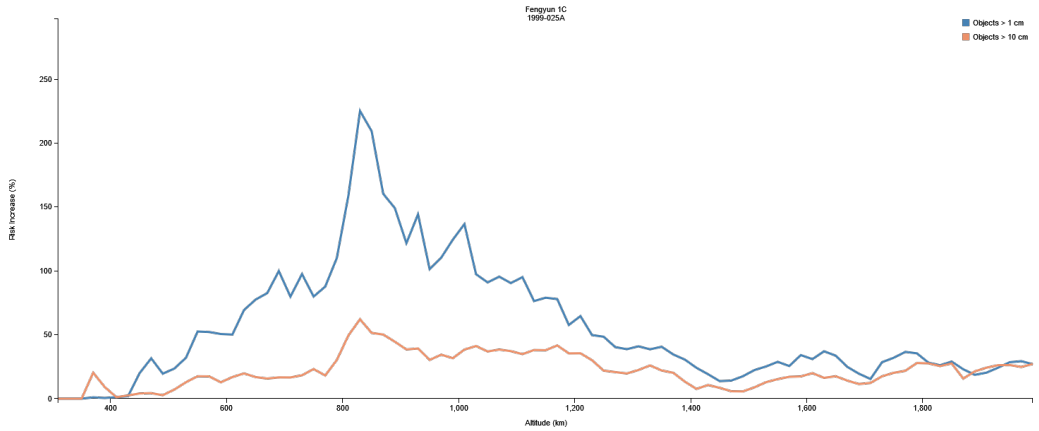

Figure 3.7: Risk increase due to the Fengyun 1C fragments in 2017. Credit: ESA

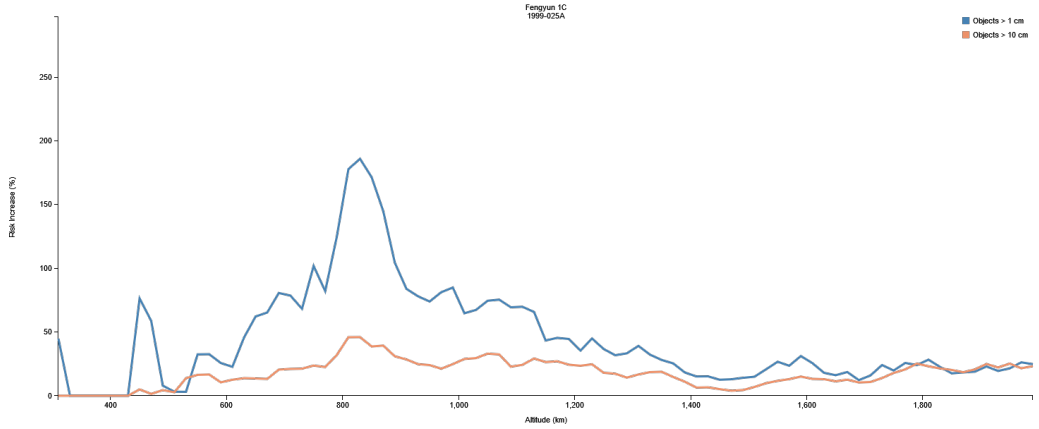

Figure 3.8: Estimated risk increase due to the Fengyun 1C fragments in 2029. Credit: ESA

Iridium 33 - Cosmos 2251 collision

On February 10, 2009, a significant event occurred in space when Cosmos 2251, which was derelict at the time of the event, and Iridium 33 collided at an altitude of around 790 km. This was the first accidental collision of two intact objects in orbit, resulting in the creation of two substantial debris

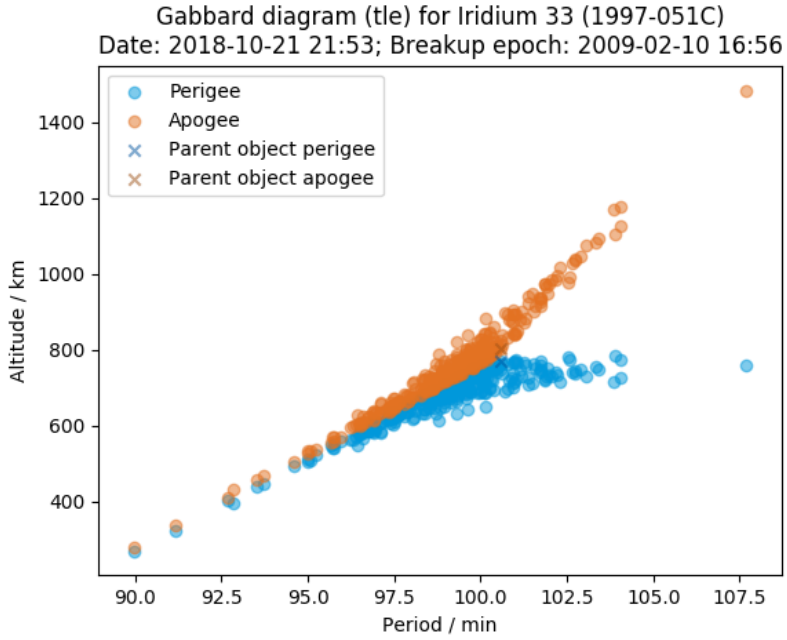

Figure 3.9: Gabbard diagram of Iridium fragments. Credit: ESA

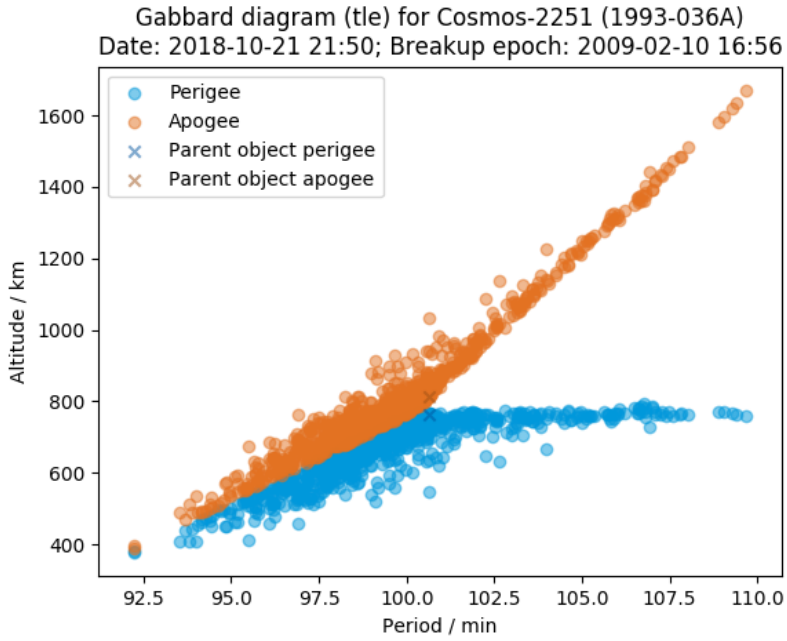

Figure 3.10: Gabbard diagram of Cosmos fragments. Credit: ESA

clouds. Both spacecraft were in nearly circular orbits with high inclinations: 86.4° and 74.0°, respectively. At the time of the collision, the two orbital planes intersected at a nearly right angle, resulting in a collision velocity of more than 11 km/s. The collision between Iridium with its 560 kg of mass and Cosmos (900 kg of mass) at the led to the production of 2370 catalogued fragments with $L_c > 10$ cm, 1330 are still in orbit.

Observations from the Haystack and Haystack Auxiliary radars have confirmed the presence of numerous small debris pieces originating from both spacecraft. Notably, Iridium has generated more debris with a higher A/m ratio, possibly due to the use of lightweight materials such as MLI and composites [23].

Although the estimates made in [24] initially predicted a faster decay rate than what has been observed, approximately 90% of cataloged collision fragments are expected to decay by 2070-2080.

Figure 3.9 and Figure 3.10 illustrate the distribution of fragments from Iridium 33 and Cosmos 2251 on the Gabbard diagram 9 years after the event, respectively. Meanwhile, Figure 3.11 and Figure 3.12 depict the increase in risk by altitude resulting from the event. This risk is evaluated with respect to the MASTER 2009 population, assuming a business-as-usual projection.

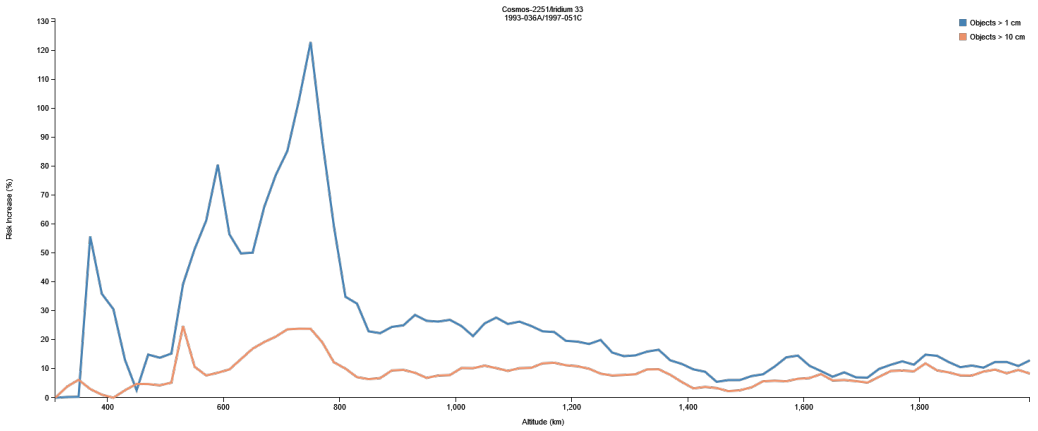

Figure 3.11: Risk increase due to the Iridium-Cosmos fragments in 2016. Credit: ESA

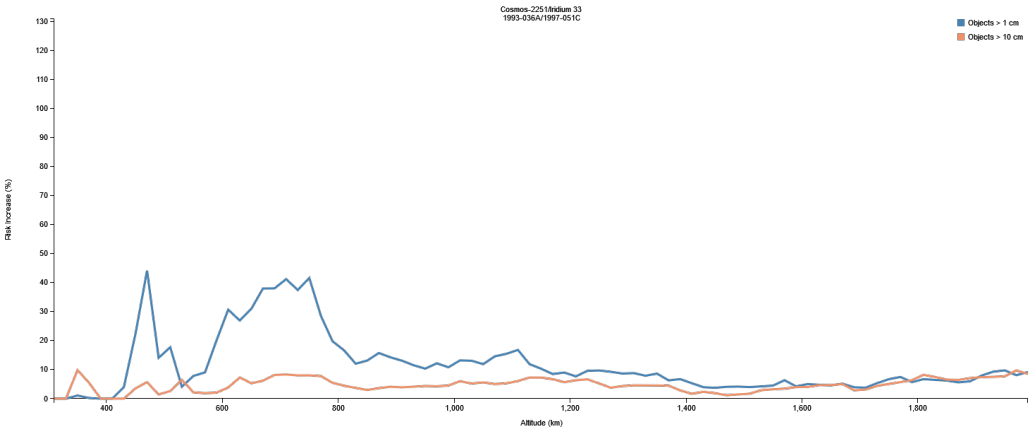

Figure 3.12: Estimated risk increase due to the Iridium-Cosmos fragments in 2029. Credit: ESA

3.2.2 Non-catastrophic breakup events

These events are included in the non-catastrophic breakup definition, generating a relatively small population of large fragments or a large population that will affect only the short term space debris environment.

Microsat-R ASAT

The Indian spacecraft Microsat-R, which was launched on January 24, 2019, underwent a deliberate destruction test as part of a ground-based ASAT weapon system experiment on March 27, 2019. At the time of its disintegration, the 740 kg spacecraft was positioned in an orbit with an apogee altitude of approximately 294 km and a perigee of 265 km and an inclination of 96.6°. As of August 8, 2019, a total of 118 debris were added to the public satellite catalog, with 55 fragments still in orbit at that date. However, it's worth noting that initially, over 400 fragments were tracked by SSN sensors. The cataloging process is complicated by the low altitude of the event and the resulting rapid orbital decay. The Gabbard plot in Figure 3.13 shows the fragments after approximately 3 months from the event.

Even if the event has generated enough large fragments to be considered a catastrophic breakup, the debris had an extremely short lifetime and didn't

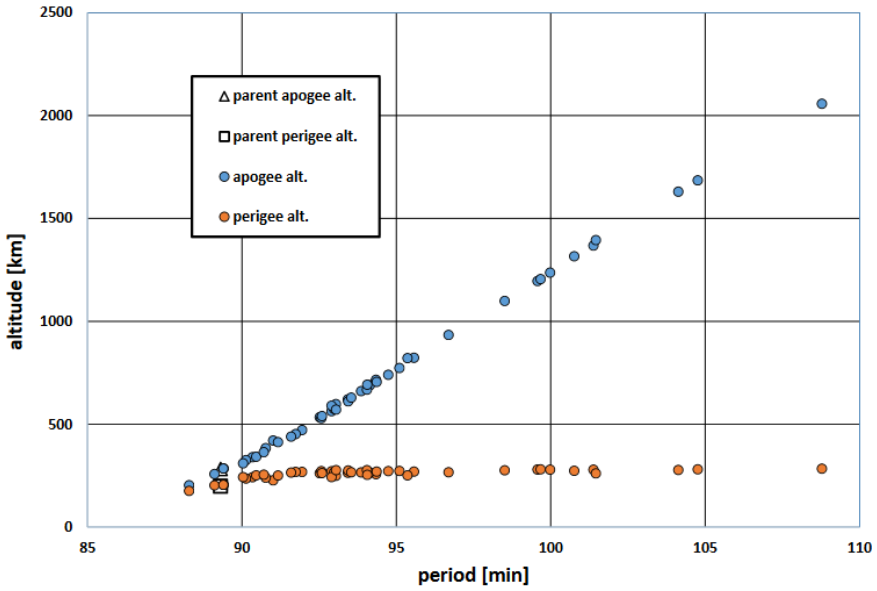

Figure 3.13: Gabbard diagram of Microsat fragments. Credit: NASA ODPO

affect the long-term space environment as shown in Figure 3.11 and Figure 3.12. The risk increase is evaluated with respect to the MASTER 2009 population, assuming a business-as-usual projection. As of November 15, 2021 only one catalogued fragment with $L_c > 10\ cm$ is still in orbit.

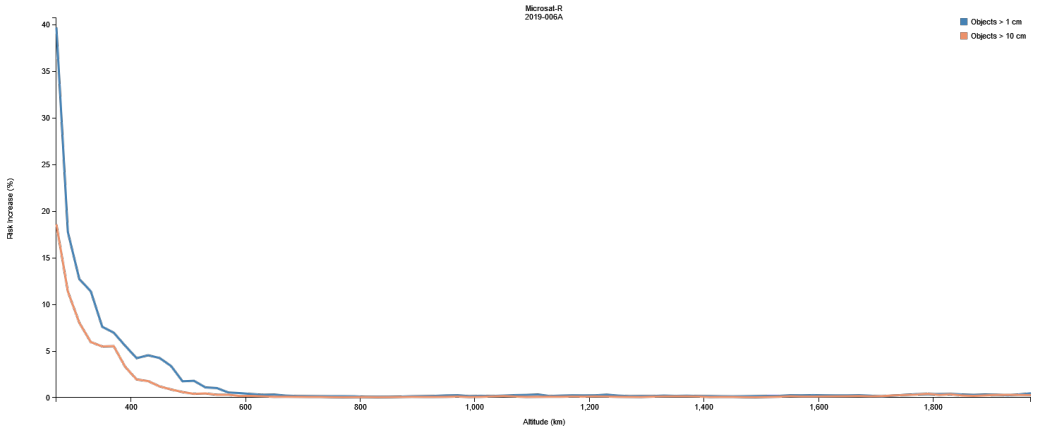

Figure 3.14: Risk increase due to the Microsat-R fragments in 2019. Credit: ESA

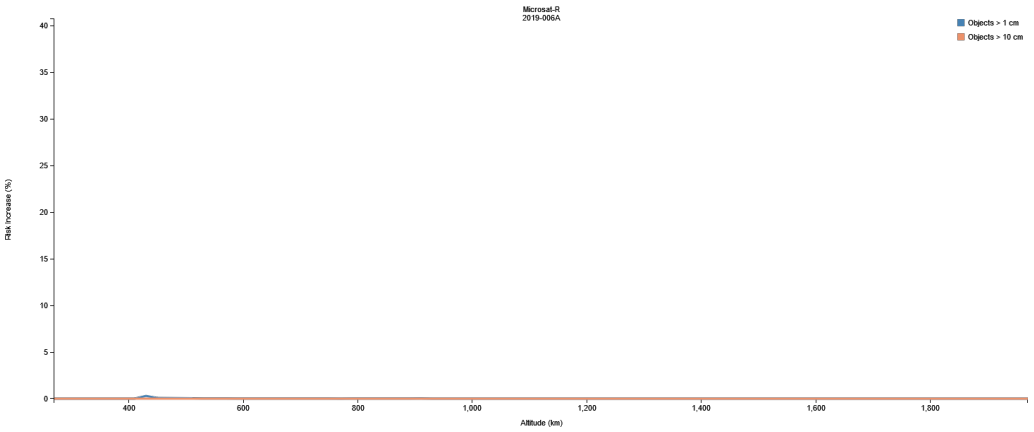

Figure 3.15: Estimated risk increase due to the Microsat-R fragments in 2024. Credit: ESA

YunHai 1-02 collision

The Chinese meteorological satellite YunHai 1-02, launched in September 2019, likely remained operational at the time of the event and thereafter. Prior to the breakup, the spacecraft was in an orbit with an apogee of 785 km and a perigee of 780 km, with an inclination of 98.54°.

As of April 22, 2023, the 18th Space Control Squadron has identified and tracked 43 fragments resulting from the breakup of YunHai 1-02. The accidental collision involved the object 1996-051Q (U.S. SSN catalog number 48078), a small mission-related debris object from the Zenit-2 rocket launched in 1996, and the YunHai satellite with a mass of approximately 800 kg. The YunHai 1-02 breakup marked the fifth confirmed accidental collision between two cataloged objects, with 33 debris from the event are still in orbit. While this event generated a relevant amount of large debris, it does not meet the criteria for being categorized as a catastrophic breakup.

Figure 3.16 illustrates the distribution of fragments related to the event on the Gabbard diagram less than one month after the event. Meanwhile, Figure 3.17 and Figure 3.18 depict the increase in risk by altitude resulting from the event. This risk is evaluated with respect to the MASTER 2009 population, assuming a business-as-usual projection.

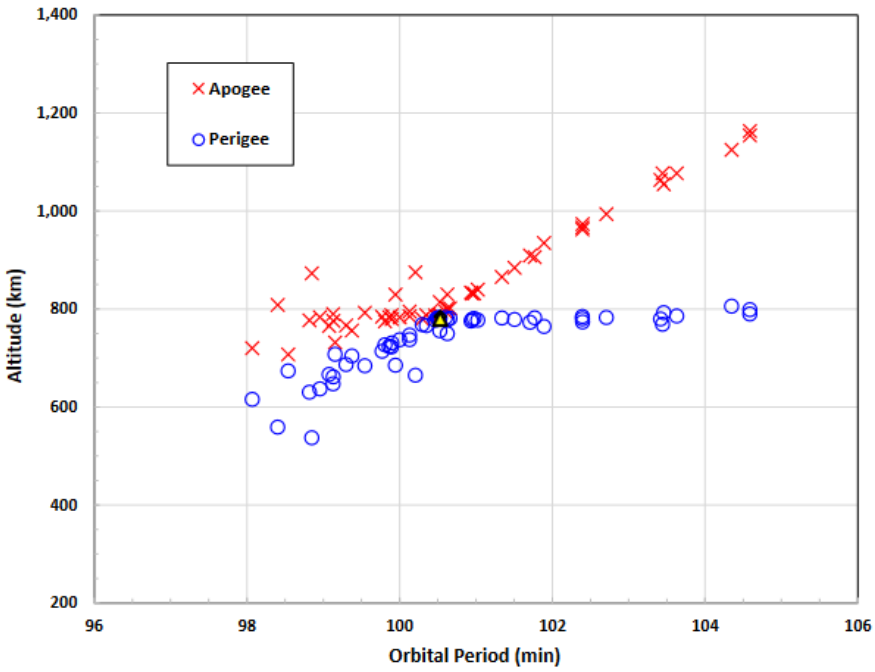

Figure 3.16: Gabbard diagram of YunHai fragments. Credit: NASA ODPO

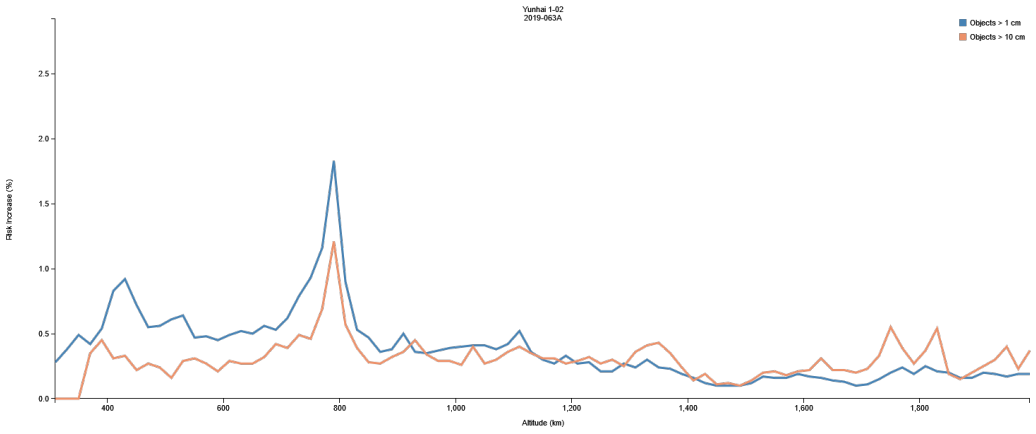

Figure 3.17: Risk increase due to the YunHai fragments in 2021. Credit: ESA

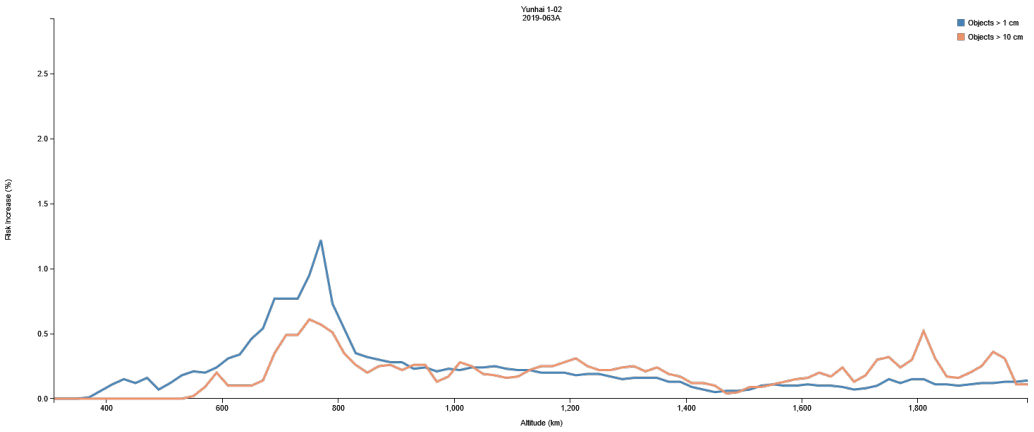

Figure 3.18: Estimated risk increase due to the YunHai fragments in 2032. Credit: ESA

3.2.3 Minor breakup events

These events are included in the minor breakup definition, generating a few large fragments that will not significantly affect the space debris environment.

CERISE collision

The incident marked the first occurrence in which two objects in the U.S. satellite catalog unintentionally collided. The CERISE spacecraft (Satellite Number 23606, International Designator 1995-033B) is a microsatellite of British design, with a mass of 50 kg. The other participant in this encounter was Satellite Number 18208 (International Designator 1986-019RF), created in November 1986 when the rocket body of ESA's SPOT 1 broke apart into nearly 500 tracked debris. The involved debris had a mass of about 4.5 kg. The orbit of this fragmentation debris at the time of the collision was in an orbit with an apogee of 680 km and a perigee of 660 km, at an inclination of 98.45°.

The collision, which occurred with a relative velocity of 14.8 km/s, resulted in the production of only two pieces of debris large enough to be tracked, which are the upper portions of the gravity-gradient boom. Analysis by the manufacturer of the spacecraft bus, Surrey Satellite Technology Ltd. at the

University of Surrey, United Kingdom, suggested that the 6-meter gravity-gradient boom had been severed at a point approximately 3.1 to 3.2 meters from its base.

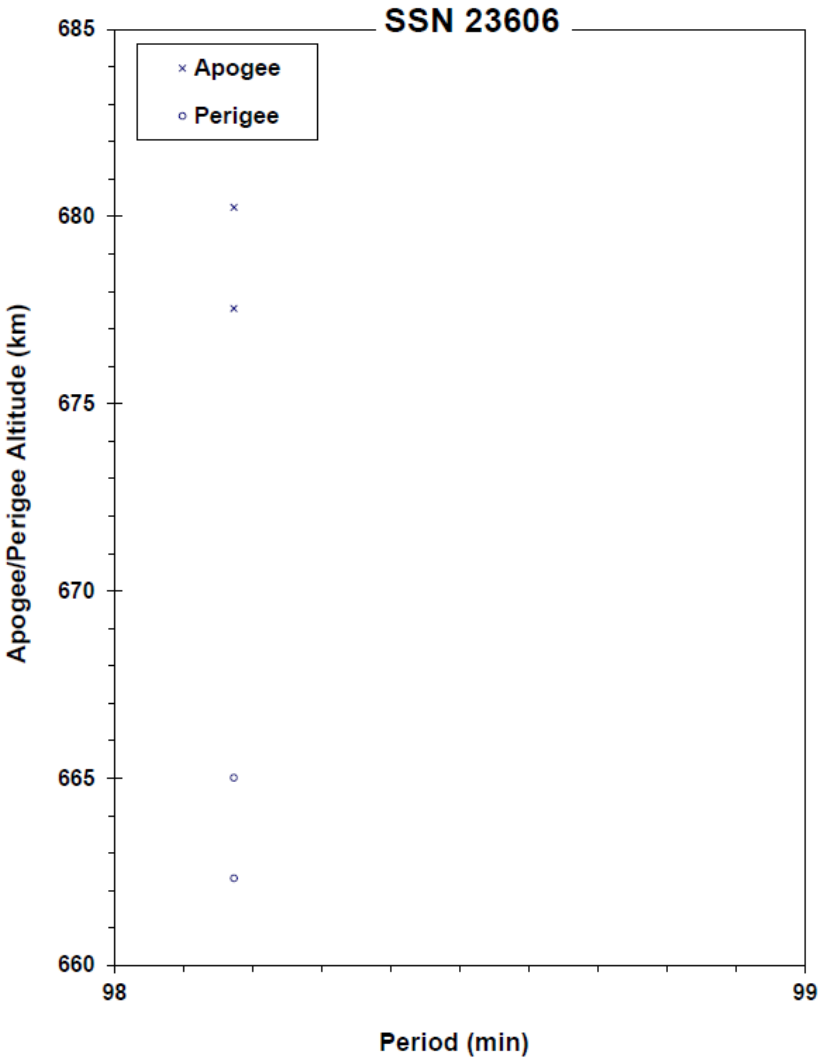

Figure 3.19: Gabbard diagram of CERISE fragments. Credit: NASA

Figure 3.19 illustrates the two fragments related to the event on the Gabbard diagram 4 days after the event. Meanwhile, Figure 3.20 and Figure 3.21 depict the increase in risk by altitude resulting from the event. This risk is evaluated with respect to the MASTER 2009 population, assuming a business-as-usual projection.

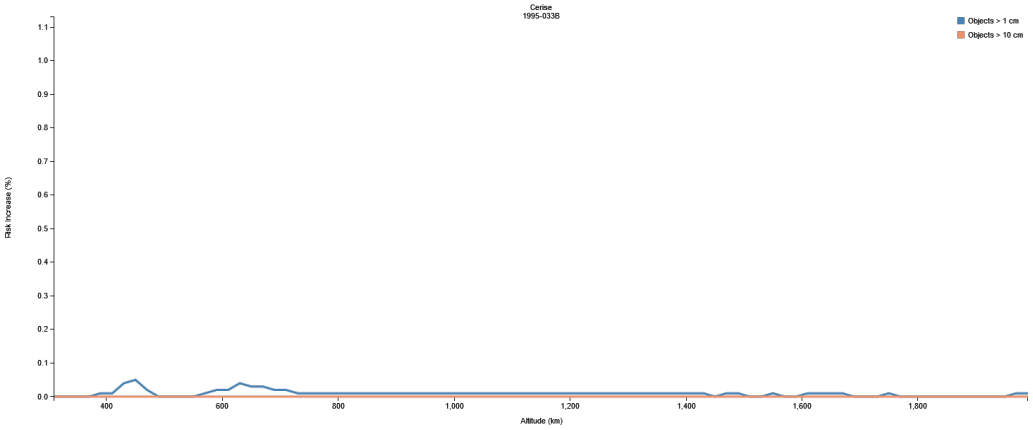

Figure 3.20: Risk increase due to the CERISE fragments in 2009. Credit: ESA

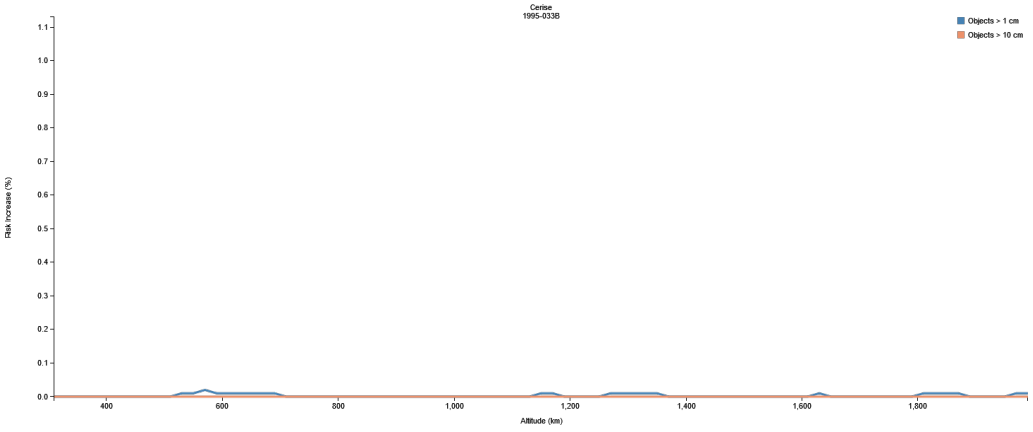

Figure 3.21: Estimated risk increase due to the CERISE fragments in 2029. Credit: ESA

3.2.4 Considerations

It's worth noting that both the EMR of the Iridium-Cosmos collision and Fengyun-1C are above the threshold. However, the same holds true for the CERISE accidental collision, which produced thousands fewer large fragments, with a mass difference of only a factor of 20. In fact, according to the NASA SBM, the CERISE collision should have produced approximately 100 fragments larger than 10 *cm*.

This highlights that the EMR cannot be the sole parameter for determining whether a collision is catastrophic or not. Relying solely on EMR would result in a substantial error in estimating debris production. As shown in Table 3.1, the accidental collisions that have occurred to date have produced a small number of fragments, even when the EMR exceeded the threshold.

Event Date	Object 1	Object 2	Cataloged Fragments
23 Dec 1991	Cosmos 1934	PM	3
24 Jul 1996	CERISE	RF	2
17 Jan 2005	THOR BURNER 2A R/B	RF	7
10 Feb 2009	Iridium 33	Cosmos 2251	2370
18 Mar 2021	YunHai 1-02	RM	43

Table 3.1: Catalogued accidental collisions

Chapter 4

Probability of a catastrophic collision

Predicting the growth of space debris is crucial for ensuring the sustainability of the space environment. While measures to mitigate explosion events involve passivation, an essential step in addressing in-orbit accidental collisions is planning mitigation strategies. To make such predictions, evolutionary models conduct complex simulations that involve assessing the probability of collisions between in-orbit objects and space debris.

The outcomes of these collisions are estimated using a breakup model, with the NASA SBM being one of the most commonly used models today. However, as discussed in Section 2.2, it's vital to acknowledge that this model has certain limitations. These limitations can introduce significant errors in the estimation of debris production, which, in turn, affects the accuracy of predictions. Therefore, these limitations must be carefully considered in the modeling process.

4.1 Proposed model

One possible way to predict the number of collisions and the probability of collision between an object and debris is by using the debris spatial density and the orbital parameters of the object under consideration. The proposed model draws inspiration from the one used in [25], incorporating an additional

coefficient to account for the limitation of the EMR threshold used. The cumulative number of collisions can be calculated as follows:

$$n = S_d(L_c) \cdot A \cdot \eta \cdot v \cdot \Delta t \tag{4.1}$$

Where:

- n is the number of impacts for a selected class of impactors
- $S_d(L_c)$ is the spatial density of the specific debris class, defined by L_c
- A is the impact cross section of the target object
- η is the additional area scaling coefficient (detailed in the next subsection)
- v is the mean relative velocity
- Δt is the time interval considered

4.1.1 Area scaling coefficient

The added area scaling coefficient η is a dimensionless number ranging from 0 to 1, serving two distinct purposes, depending on the type of collision considered:

1. It addresses the overestimation of the number of catastrophic collisions predicted by evolutionary models. This overestimation results from the limitation of using only the EMR as a parameter to determine whether a collision is catastrophic or not. As demonstrated in previous sections, some recorded events with an EMR > 40 J/g resulted in a very low number of fragments, likely because the impacts were not central. The area scaling coefficient is employed to filter out non-central impacts.

2. It deals with impacts that involve specific portions of the target object. This can account for potential cases of induced breakup or the loss of PMD capabilities due to a collision. Induced breakups occur when

non-passivated energy sources, such as pressurized tanks, residual propellants, or charged batteries, are present, and a trigger condition can initiate an explosive event, such as a collision. On the other hand, the loss of PMD capabilities due to a collision occurs when a critical component loses its specific function of deorbiting the spacecraft. In such cases, the area scaling coefficient filters out impacts that do not involve the selected critical parts.

The coefficient is defined as follows:

$$\eta = \frac{A_{cr}}{A} \tag{4.2}$$

Where A_{cr} is one of the following, depending on the case:

1. The critical cross section in which the EMR threshold and Equation (2.7) are applicable for estimating the number of fragments produced.

2. The cross section of the critical component in exam.

While A is the total impact cross section of the target object.

Once the number of collisions is calculated with Equation (4.1), the Poisson distribution can be employed to assess the probability of the event.

4.1.2 Poisson distribution

The Poisson distribution is a probability distribution that describes the number of events that occur in a fixed interval of time or space. It is often used when the events are rare and random (the events happen independently of the time since the last event), and the average number of events in the given interval is known.

$$P(k) = \frac{e^{-\lambda}\lambda^k}{k!} \tag{4.3}$$

Where:

- $P(k)$ is the probability of observing k events.

- λ is the average rate of event occurrences in the given interval.
- k is a non-negative integer representing the number of events.

For the purpose of this thesis, the probability of a single collision is investigated, setting $k = 1$ and $\lambda = n$. The equation becomes:

$$P = 1 - \exp(-n) \tag{4.4}$$

4.2 Envisat case study

As an example, a collision with the derelict Envisat is considered, as it is a known potential source of space debris. Launched on March 1, 2002, aboard an Ariane-5 rocket from Europe's spaceport in French Guiana, Envisat held the distinction of being the largest Earth observation spacecraft ever constructed. After a decade of operation, its mission concluded on April 8, 2012, due to an unexpected loss of contact.

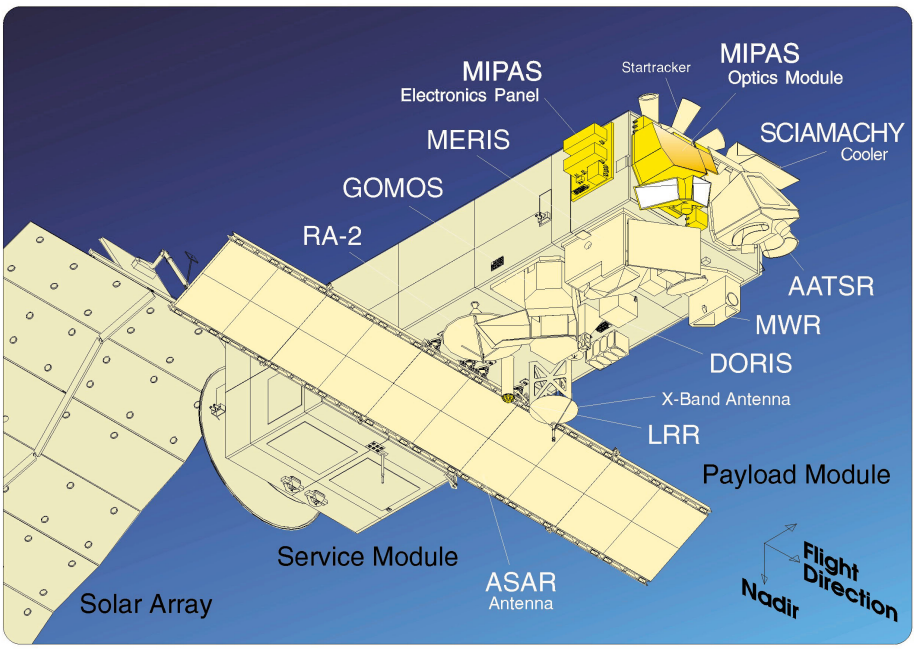

Figure 4.1: Envisat. Credit: ESA

Using the model introduced in the preceding section, this section delves into the exploration of three distinct collision categories, all centered around Envisat as the target object. The objective is to evaluate the probability of catastrophic consequences. These collision types include:

1. Catastrophic collision resulting in an EMR exceeding 40 J/g, as defined by the NASA SBM. In this case, the minimum debris dimension chosen for spatial density calculation is the one that can reach the EMR threshold. The area scaling coefficient, denoted as η, is applied to account for direct impacts while disregarding appendices and glancing impacts.

2. Collision with an EMR less than 40 J/g but still leading to a catastrophic breakup for the space environment. For instance, this may involve the production of more than 100 debris pieces with $L_c > 10$ cm (as defined in Section 3.1). The selected minimum debris dimension for spatial density calculation is the one that can result in a catastrophic breakup. Similar to the first scenario, the area scaling coefficient (η) is used to consider only direct impacts and exclude appendices and glancing impacts.

3. This scenario concerns an induced breakup resulting from the collision and the presence of non-passivated energy sources. This approach is also applicable to cases involving the loss of PMD capabilities. However, in the specific case of Envisat, it had already lost its PMD capabilities and was not passivated before the loss of contact. Therefore, the induced breakup scenario is considered. The minimum debris dimension chosen for spatial density calculation is the one that can penetrate the target's shielding and damage critical internal components. In this case, the area scaling coefficient (η) is employed with a focus on critical components such as tanks or batteries.

Envisat now resides in a circular orbit at approximately 760 km altitude, with a 100-minute orbital period and an inclination of 98°. The satellite has a mass of 8000 kg, and with its solar array fully deployed, it stretches to a

total length of 26 m. The primary structure, consisting of the payload and service module, can be enclosed in a cylinder measuring 5 m in diameter and 10 m in height. The main cross section of Envisat is so considered 50 m^2.

For the first two cases, to address the possibility of overestimating catastrophic collisions, the area scaling coefficient is set to 0.5, as suggested in [9].

Then, for the third case the service module is considered as the critical component, as it can cause an induced breakup. So the impact cross section of the service module for the "induced breakup" case is approximately 9.8% of the main structure's cross section [26] and the area scaling coefficient is set consequently.
For this example, several assumptions have been made. It is assumed that the orbit and the debris population remain constant, with the chosen population being the latest observed on MASTER 8 (01/11/2016) as illustrated in Figure 4.2, Figure 4.3 and Figure 4.4.

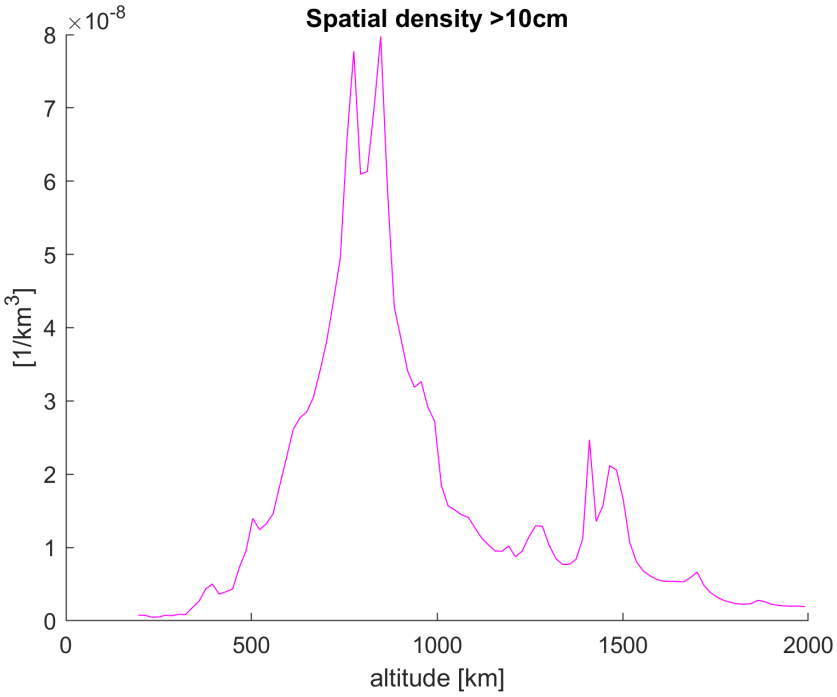

Figure 4.2: MASTER 8 LEO spatial density of debris larger than 10 cm

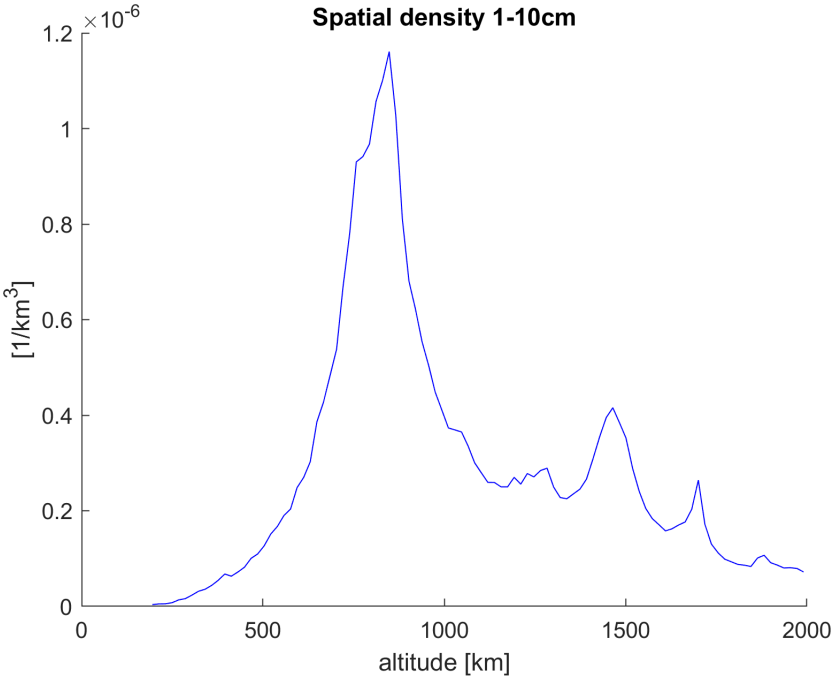

Figure 4.3: MASTER 8 LEO spatial density of debris from 1 to 10 *cm*

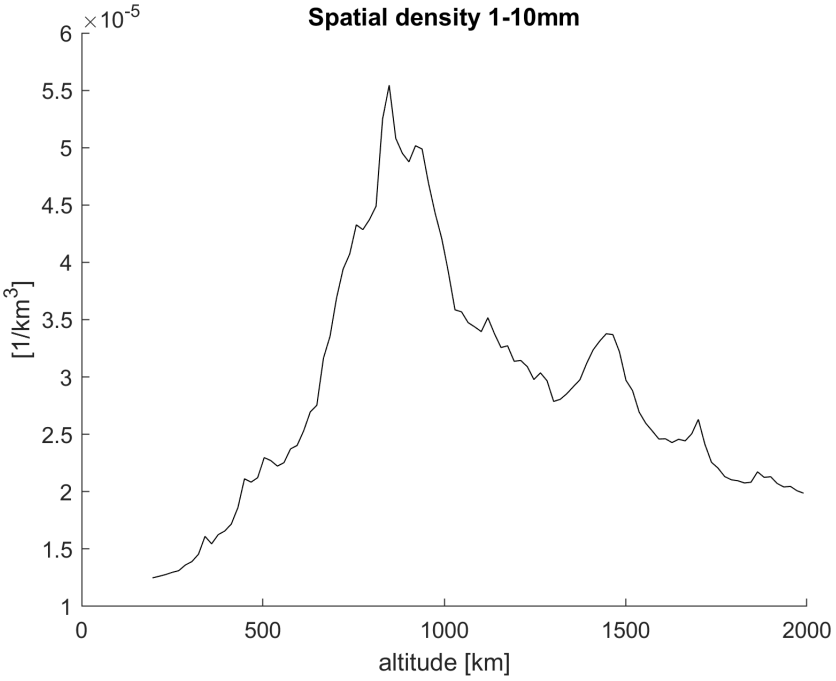

Figure 4.4: MASTER 8 LEO spatial density of debris from 1 to 10 *mm*

An average impact velocity of 10 km/s has been selected. The number of collisions is calculated for one year in orbit.

4.2.1 Analysis results

Using the provided model and the previously mentioned hypotheses, here are the resulting consequences and their associated probabilities:

Case 1: catastrophic EMR

As illustrated in Figure 4.5 the complete fragmentation of Envisat could be one of the most severe events for the space environment, producing more than 4000 fragments according to the NASA SBM. The catastrophic threshold is reached with a spherical debris diameter of 40 cm, following the concept of diminishing density (Equation (2.3)).

Taking into account all the preceding assumptions, the annual collision rate capable of causing the complete fragmentation of Envisat is 8.01e-5. This results in a collision probability that remains just below the collision avoidance warning threshold of 1/10000 [27]. However, when extending the time interval to two years, the collision probability surpasses the quoted threshold. Since Envisat is not expected to reenter the atmosphere in the near future, it's prudent to contemplate a 100-year interval. In this case, the probability increases to 8e-3. Therefore, over the next 100 years, there is an 0.8% probability that a collision with Envisat will generate more than 4000 new fragments.

Case 2: catastrophic breakup

Similarly, as depicted in Figure 4.5, a 10 cm debris based on the same concept, has the potential to generate a significant number of larger fragments, exceeding 100, without reaching the catastrophic EMR threshold.

The annual collision rate that can lead to the catastrophic breakup of Envisat, generating more than 100 debris pieces, is 5.19e-4. This results in a

collision probability that surpasses the collision avoidance warning threshold. When considering the same 100-year time interval as in the previous case, the probability of a catastrophic breakup rises to 0.0506. Therefore, over the next 100 years, there is a 5.06% probability that a collision with Envisat will produce more than 100 new fragments.

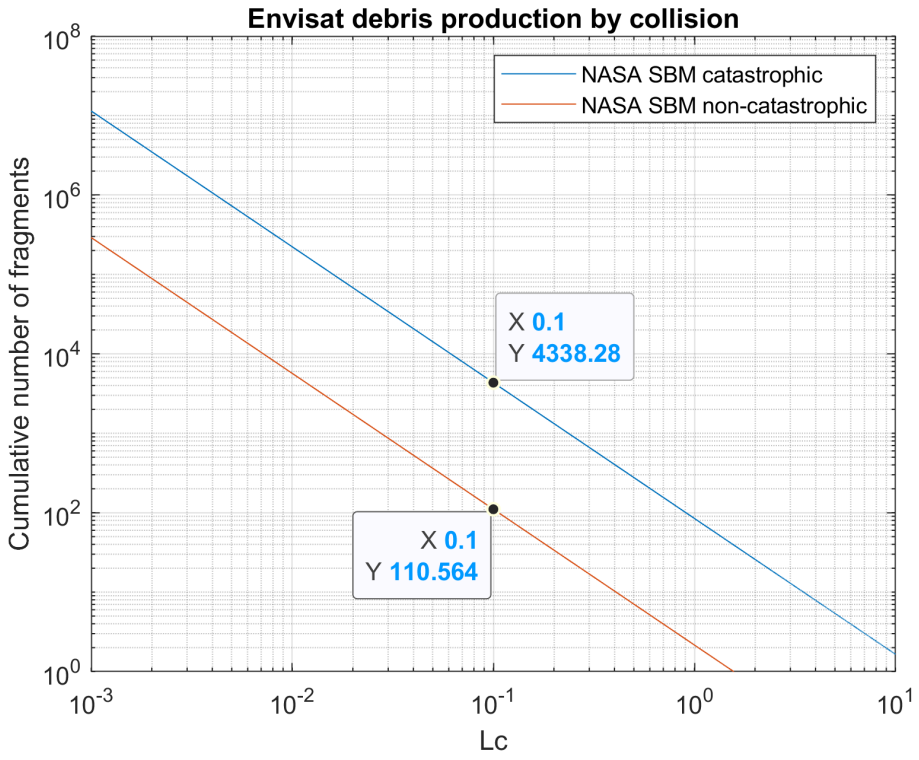

Figure 4.5: Modeled debris production: Envisat collision

Case 3: catastrophic induced-breakup

In the case of Envisat, which has already lost its PMD capabilities, the service module is considered a critical component. This module could potentially contain residual energy from propellant remnants or charged batteries. An impact could trigger an explosive event that might lead to a catastrophic breakup, as shown in Figure 4.6, assuming a scaling factor (s) of 0.5 for the Equation (2.5). It is important to note that a prior value for this scaling factor is not possible to determine as Envisat is a unique case in terms of

mass and dimensions.

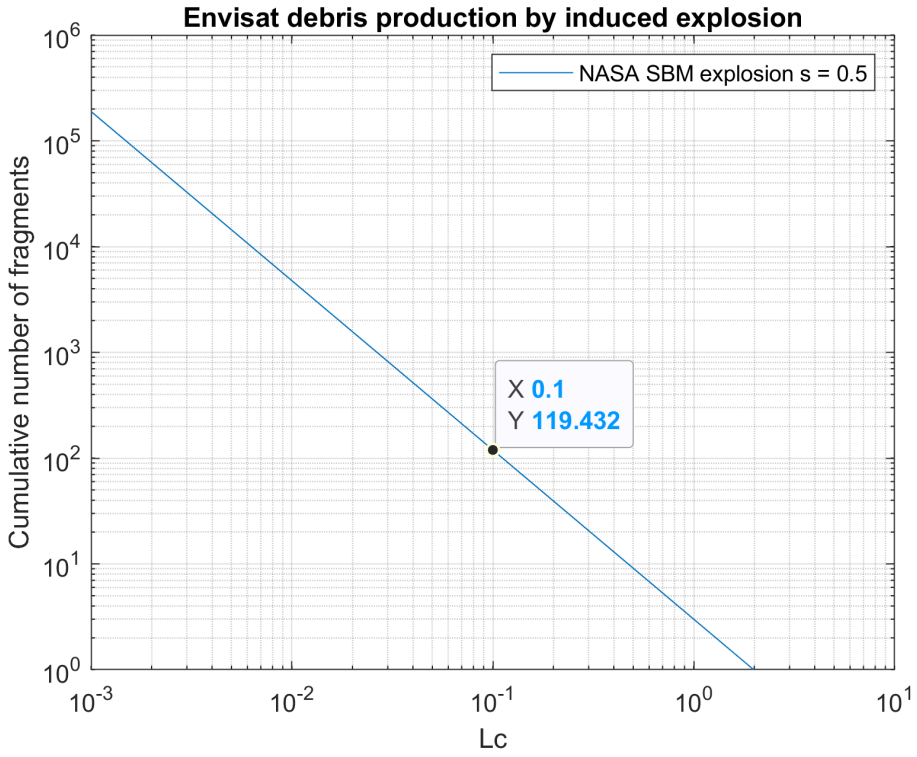

Figure 4.6: Modeled debris production: Envisat explosion

To assess the collision probability, the minimum debris size for spatial density calculation needs to be chosen. At a relative velocity of 10 km/s, debris larger than 1 mm is unlikely to penetrate an aluminum monolithic shield as in Figure 4.7. For an explosion to occur, the collision debris would typically need to breach the external structure of the service module and puncture the propellant tank, potentially containing remnants of the 319 kg of hydrazine loaded at the beginning of life. However, due to unknowns regarding the internal layout and the type of shielding, a debris size of 5 mm is assumed to be capable of perforating the tank and inducing an explosion. This size is chosen based on its potential to breach the Whipple shield shown in Figure 4.7, which is assumed representative of the protections of a large satellite such as Envisat.

The annual collision rate that can lead to an induced breakup of Envisat is

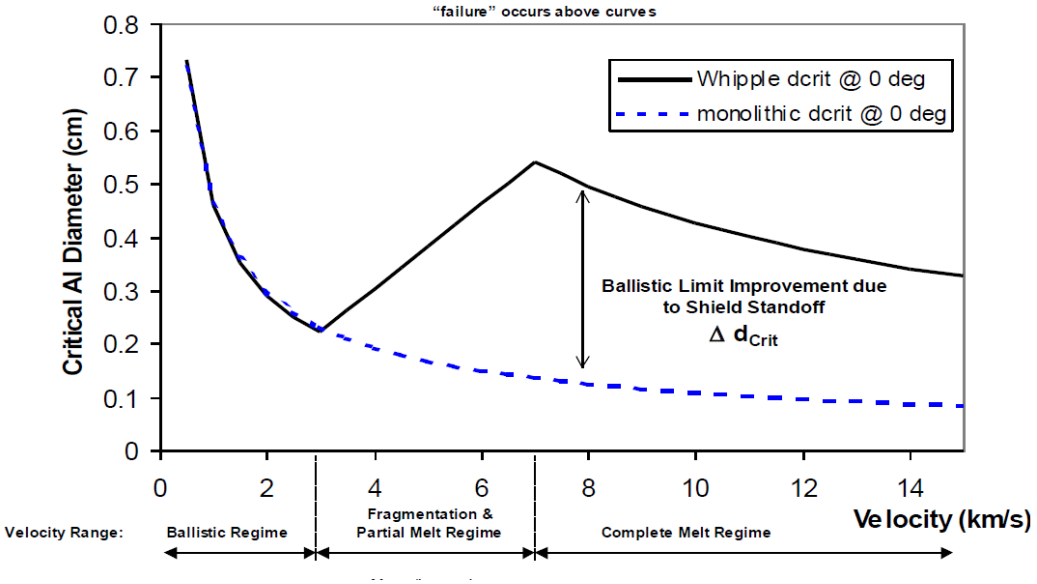

Figure 4.7: Ballistic limit for spacecraft shielding. Failure criterion is threshold perforation or detached spall from rear wall. Monolithic target is 0.44 *cm* thick Al 6061T6. Whipple shield consists of 0.12 *cm* thick Al 6061T6 bumper followed at 10 *cm* by 0.32 *cm* thick Al 6061T6 rear wall [3]

4e-3. This results in a collision probability that exceeds the collision avoidance warning threshold by more than an order of magnitude. When considering the same 100-year time interval as in the previous cases, the probability of an impact with debris potentially capable of inducing an explosion rises to 0.332. Therefore, over the next 100 years, there is a 33.2% probability that a collision of Envisat with debris large enough has the potential to induce an explosion.

4.3 COSMO-SkyMed case study

The COSMO-SkyMed (CSK) constellation, an Italian Earth-imaging system, comprises four identical satellites launched between 2007 and 2010. As of now, CSK-1, CSK-2, and CSK-4 continue to be in operational status. The acronym COSMO-SkyMed represents "COnstellation of small Satellites for the Mediterranean basin Observation". This mission is under the ownership and operation of the Agenzia Spaziale Italiana (ASI), with funding support

from the Italian Ministry of Research and the Italian Ministry of Defense [28].

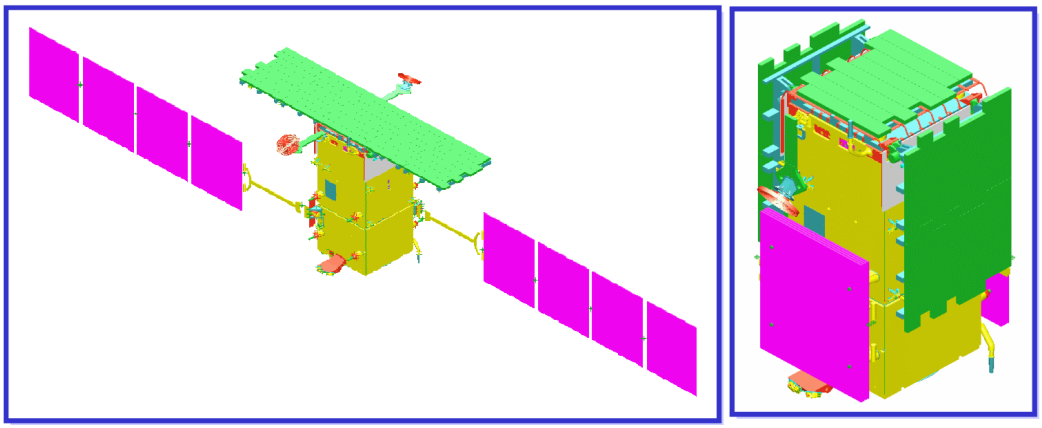

Figure 4.8: COSMO-SkyMed deployed and stowed configurations. Credit: ASI

Using the same approach applied to Envisat, this section delves into the exploration of the same three distinct collision categories, this time centered around SkyMed-1 as the target object. The objective is to evaluate the probability of catastrophic consequences. The collision types include:

1. Catastrophic collision resulting in an EMR exceeding 40 J/g, as defined by the NASA SBM. In this case, the minimum debris dimension chosen for spatial density calculation is the one that can reach the EMR threshold. The area scaling coefficient, denoted as η, is applied to account for direct impacts while disregarding appendices and glancing impacts.

2. Collision with an EMR less than 40 J/g but still leading to a catastrophic breakup for the space environment. For instance, this may involve the production of more than 100 debris pieces with $L_c > 10$ cm (as defined in Section 3.1). The selected minimum debris dimension for spatial density calculation is the one that can result in a catastrophic breakup. Similar to the first scenario, the area scaling coefficient (η) is used to consider only direct impacts and exclude appendices and glancing impacts.

3. This scenario concerns an induced breakup resulting from the collision and the presence of non-passivated energy sources. This approach is also applicable to cases involving the loss of PMD capabilities. Since the satellite is still operational, so both induced breakup and loss of PMD scenarios are discussed. The minimum debris dimension chosen for spatial density calculation is the one that can penetrate the target's shielding and damage critical internal components. In this case, the area scaling coefficient (η) is employed with a focus on such critical components.

Skymed-1 resides in a nearly circular orbit at approximately 620 km altitude, with a 97-minute orbital period and an inclination of 97.86°. The satellite has a mass of 1700 kg, with the cross section of the main bus of about 7.98 m^2 while the solar arrays fully deployed have a cross section of 18.3 m^2.

As with Envisat, in the first two cases, to mitigate the possibility of overestimating catastrophic collisions, the area scaling coefficient is set to 0.5.

Then, for the third case, the pressurized tank is considered as the critical component for an explosion, as it can cause an induced breakup. The tank geometry is spherical with a cylindrical intersection and has a cross section of about 0.366 m^2. So the impact cross section of the pressurized tank for the "induced breakup" case is considered 4.59% of the main structure's cross section, and the area scaling coefficient is set accordingly.
For the loss of PMD capabilities, the Piattaforma Riconfigurabile Italiana Multi Applicativa (PRIMA) Bus is considered the critical component. It has a cross section of about 1.96 m^2, representing the 24.6% of the main structure's cross section. The area scaling factor is set accordingly.

As in the last section, it is assumed that the orbit and the debris population remain constant, with the chosen population being the latest observed on MASTER 8 (01/11/2016) as illustrated in Figure 4.2, Figure 4.3 and Figure 4.4. The average impact velocity is 10 km/s and the number of collisions is calculated for one year in orbit.

4.3.1 Analysis results

As before, using the provided model and the previously mentioned hypotheses, here are the resulting consequences and their associated probabilities:

Case 1: catastrophic EMR

As illustrated in Figure 4.9 the complete fragmentation of SkyMed-1 could produce more than 1300 fragments, according to the NASA SBM. The catastrophic threshold is reached with a spherical debris diameter of 20 *cm*, following the concept of diminishing density (Equation (2.3)).

Taking into account all the preceding assumptions, the annual collision rate capable of causing the complete fragmentation of SkyMed-1 is 1.8e-5. When extending the time interval to 15 years, which is the time the satellite has already spent in orbit, the collision probability rises to 2.7e-4.

Case 2: catastrophic breakup

Similarly, as depicted in Figure 4.9, a 10 *cm* debris based on the same concept, has the potential to generate a significant number of larger fragments, exceeding 100, without reaching the catastrophic EMR threshold.

The annual collision rate that can lead to the catastrophic breakup of SkyMed-1, generating more than 100 debris pieces, is 3.3e-5. When considering the same 15-year time interval as in the previous case, the probability of a catastrophic breakup rises to 5.1e-4.

Both of the analyzed cases (Case 1 and Case 2) result in a probability above the warning threshold for collision avoidance. However, the SkyMed-1 satellite is still operational and both scenarios involve projectiles larger than 10 *cm*, which are assumed to be catalogued and tracked in LEO. Therefore, it is reasonable to anticipate that collision avoidance measures would have effectively prevented possible encounters between the satellite and catalogued objects.

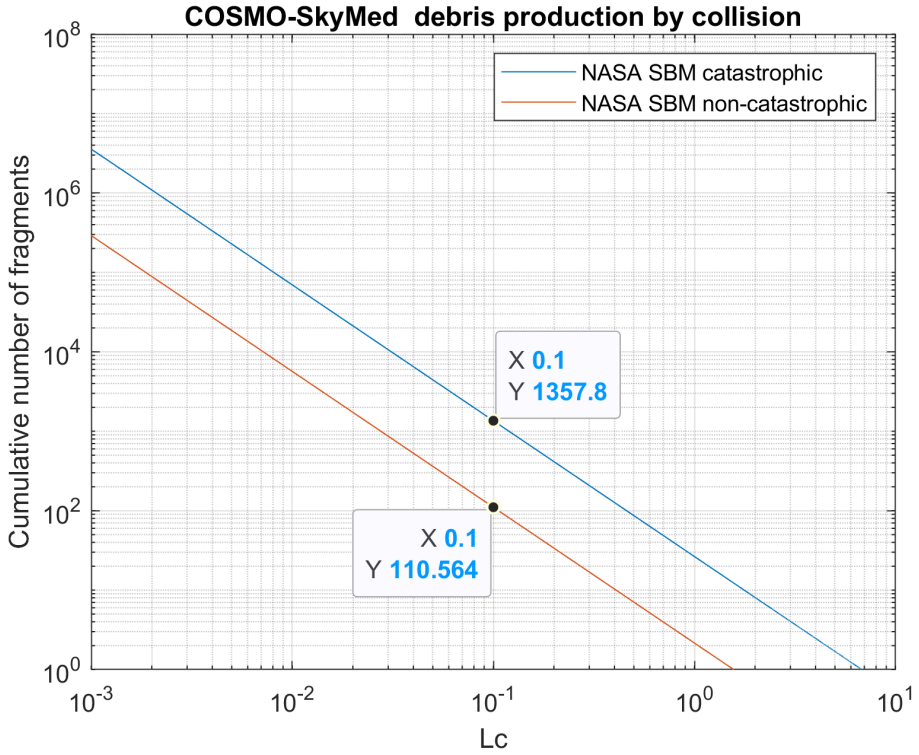

Figure 4.9: Modeled debris production: COSMO-SkyMed collision

Case 3: catastrophic induced-breakup / loss of PMD capabilities

As with the Envisat example, determining the scaling factor for the explosion is not possible since there's no recorded explosion of this satellite type. The NASA SBM for explosions is an empirical model not dependent on mass, and the outcome entirely depends on the scaling factor. A scaling factor (s) of 0.5 for the Equation (2.5) would lead to the same debris production shown in Figure 4.6.
On the other hand, a collision with a large enough debris can damage internal components in the PRIMA bus and leave a large derelict in orbit.

To assess the collision probability, the minimum debris size for spatial density calculation must be chosen. Assuming that the same hypotheses made for Envisat remain valid for SkyMed-1, a debris size of 5 mm is selected for both the induced breakup case and the loss of PMD capabilities.

The annual collision rate that can lead to an induced breakup of SkyMed-1 is 1.10e-4. This results in a collision probability that barely exceeds the collision avoidance warning threshold. When considering the same 15-year time interval as in the previous cases, the probability of an impact with debris potentially capable of inducing an explosion rises to 1.55e-3.
Instead, the annual collision rate capable of damaging the bus and causing the loss of PMD capabilities is 5.52e-4, while the probability rises to 8.25e-3 over the 15 year in orbit.

4.4 Considerations

One of the assumptions is to maintain a constant debris spatial density. Therefore, it's important to acknowledge that these collision rates and probabilities are likely to increase over time as the debris population grows. As demonstrated in the previous sections, the probabilities of collision with smaller debris, under 10 cm, are significantly greater than the probabilities of collision with larger fragments. This is a critical range because it is not covered by collision avoidance or shielding.

It's important to note that this analysis does not account for impacts with appendices, such as antennas and solar panels, as their consequences would not be as severe as those considered. Additionally, the case of a glancing impact is not addressed because there is no empirical model available for estimating the fragments generated in such scenarios, and using the NASA SBM could introduce considerable errors in the estimation. However, the probability of collision could be assessed using a complementary area scaling coefficient $(1 - \eta)$ instead of η.

The utilization of this area scaling coefficient could potentially help offset the overestimation of the number of catastrophic collisions predicted in evolutionary models. Naturally, this coefficient would require validation through simulations and tests involving both catastrophic and non-catastrophic EMR values in non-central impact scenarios.

Chapter 5

Conclusions

This chapter addresses mitigation strategies for catastrophic breakups and concludes the thesis with an emphasis on potential future research to enhance our understanding of such events.

5.1 Mitigation strategies

The most effective way to mitigate the increasing collision trend is surely the reduction of the uncontrolled objects in the near-Earth orbits. Various strategies are available for managing and mitigating the growth of orbital debris. However, the current emphasis lies in shaping the future space environment rather than significantly altering the existing debris situation. There are three primary generic approaches to debris control: design improvements, disposal, and active removal. Another supplementary mitigation approach includes collision avoidance, which can be applied to maneuverable operational spacecraft and rocket stages.

5.1.1 Design improvements

Enhancing space vehicle design involves several key aspects. Firstly, it encompasses the design of payloads and rocket bodies with the aim of minimizing or completely avoiding the release of space debris during regular operations. When mission debris release is unavoidable, efforts are made to

minimize the quantity, surface area, and orbital lifetime of the debris. This may involve designing launch vehicles and spacecraft to dispose of separation devices, payload shrouds, and other expendable components at altitudes and velocities that prevent them from entering orbit. Complexities arise when multiple spacecraft share a common launch vehicle, but the use of lanyards and similar mechanisms helps minimize potential debris generation.

The second aspect focuses on enhancing the reliability of space systems in all operational regimes. The goal is to reduce the likelihood of breakups during mission phases through a thorough analysis of failure scenarios, improved subsystem reliability, and mitigation of the risk of post-mission breakups caused by stored energy or intentional destructive actions. This includes designing boosters and payloads to prevent spontaneous explosions of rocket bodies and spacecraft. For stages and spacecraft lacking active deorbiting capabilities, efforts are made to render them inert by expelling propellants, pressurizing gases, and guarding against battery overcharging through design modifications.
In the past, spacecraft design only considered the natural meteoroid environment, but today, it takes into account the additional hazards presented by human-made orbital debris. This involves shielding energized systems, passivating energized systems, and addressing known design flaws to prevent future explosion events. Similarly, the ability to de-energize systems once a spacecraft or rocket body is no longer functional is crucial. This approach was not consistently applied until after a series of rocket body explosions occurred long after payload delivery, prompting design changes that significantly reduced the risk of such explosions.

5.1.2 Disposal

Disposal or deorbiting of spent upper stages and spacecraft represents a more proactive strategy than passivation. It involves executing perigee-lowering maneuvers to limit the object's orbital lifetime to a minimum threshold, typically around 25 years. This maneuver efficiently moves the object away from high collision risk regions and removes mass from orbit much faster than

if left unaltered. Alternatively, relocating derelict rocket bodies to orbital regions with fewer active spacecraft, such as the region between 2000 km altitude and GEO, can effectively safeguard the LEO environment for future missions.

The 25 year rule

Reducing congestion in the LEO environment is best achieved by imposing a limit on the lifetime of objects below 2000 km. This approach offers a two-fold benefit: objects spend less time in LEO, reducing their exposure to collision or explosion risks. Most international standards recommend a 25-year maximum post-mission lifetime for newly launched objects in LEO. However, this rule wasn't consistently applied until recent decades, so the positive effects are only beginning to emerge.

Storage orbits

As the GEO regime is situated at a considerable altitude, it is impractical to reenter spacecraft once they have reached the end of their operational lifetime. Instead, a feasible approach involves relocating these objects away from the GEO belt, making them available for potential future missions. Extensive studies have been conducted to determine the precise altitude adjustment required to prevent these objects from reentering the GEO belt due to perturbing forces, such as solar radiation pressure and lunar perturbations. The object's A/m ratio can affect the necessary altitude, with the typical requirement being at least 200 km above GEO, and often up to 300 km above. Minimizing the eccentricity of the orbit is equally important. Long-term orbit predictions are vital to ensure that the object remains outside the GEO regime for extended periods, typically over 100 years.

Storage orbits can also be established between LEO and GEO, provided that the perigee remains above 2000 km, and the apogee does not pose a threat to the GEO regime. Typically, the apogee should be at least 200 km below GEO, with the perigee at or above 2000 km.

Controlled reentry

A highly effective but costly and technically challenging method for reducing debris in LEO is direct and controlled reentry upon completing a mission. However, this approach can be complex and may require additional fuel and entail risks related to system functionality. Controlled reentry is mainly necessary when a large satellite is not expected to naturally demise upon atmospheric reentry. Therefore, sufficient fuel reserves must be left to guide the object to unpopulated areas, typically the ocean. Although expensive, controlled reentry eliminates long-term on-orbit fragmentation risk by reducing the object's orbital lifetime to its mission lifetime.

5.1.3 Active Debris Removal

While improvements in mission and hardware design will assist in addressing the orbital debris problem, this alone may not be sufficient to prevent orbital debris population growth as seen in Section 2.3. Even without further launches, debris-producing collisions could gradually add to the population count over time. This prompts consideration of programs for active debris removal to fully control the orbital debris issue. Debris remediation discussions pertain primarily to LEO, as there is presently no need for a removal system at GEO.

Active removal, while not currently economically viable, is another avenue for mitigating debris. This approach involves targeting specific objects with the highest mass or the highest risk of explosion and removing them from orbit through rendezvous or retrieval systems. Although the cost of such endeavors is currently a challenge, it is acknowledged that active removal may become a viable debris mitigation technique in the future. This technique is also the only one that directly addresses the mitigation of intact derelicts already in orbit, which can potentially collide with other debris fragments, as exemplified in the Envisat case discussed in Section 4.2. Currently, only demonstrative missions are in progress [29] [30], so this technique will be a valuable option only for future decades.

Removing large inert objects necessitates an active maneuver vehicle capable of rendezvousing with, grappling, and accurately applying the required velocity increment to move inert, tumbling, and non-cooperative targets to a desired orbit. As stated earlier, no uninhabited system currently demonstrated these capabilities. Developing a maneuverable stage for the removal of other stages and spacecraft requires a high degree of automation in rendezvous, grapple, and entry burn management to maintain practical operating costs. Instead, removing fragmented objects individually would be less practical and is not a concrete possibility in the near future.

5.1.4 Collision avoidance

Collision avoidance serves as a complementary measure, applicable only during conjunctions between operational objects with a propulsion system and cataloged debris. This technique relies on the availability of TLE, which may lack the precision required for accurate calculations. Data accessible to the public through the Space-Track website typically come in the form of general perturbation mean element sets rather than the more precise osculating orbital parameters.

Given that current shielding technology is primarily effective for objects with a diameter of 1 cm or less, the ability to detect and track objects as small as 1 cm becomes crucial in bridging the gap between collision avoidance and shielding as risk mitigation strategies. However, the population of objects sized between 1-10 cm is roughly an order of magnitude greater than those larger than 10 cm, highlighting the necessity of enhancing both detection capabilities and data processing.

5.2 Thesis conclusion

This work presents a comprehensive examination of the phenomenon of catastrophic fragmentation and its significant impact on the space environment compared to more frequent minor events. Through an analysis of historical

data, it provides insights into the composition of the space debris environment concerning cataloged objects with sizes greater than 10 cm.

The study reevaluates the concept of "catastrophic fragmentation", particularly the catastrophic collision as defined by the NASA SBM. This is of utmost importance for the modeling community dedicated to simulating the long-term evolution of the orbital debris environment. The study offers a refined definition of "catastrophic breakup" that focuses on its effects on the debris population, taking into account aspects such as debris production, fragmented mass, and in-orbit duration to classify breakup types with clear and straightforward thresholds. These chosen thresholds aim to provide a comprehensive overview of the events that have most significantly influenced the current fragment population.
As outlined in Chapter 3, the mere production of debris is not considered catastrophic if the orbital lifetime of these fragments is sufficiently short. This approach enables the characterization of past events that have contributed to the increase of fragmentation debris.

Analyzing cataloged collisions revealed some discrepancies with the fragmentation model. Despite all recorded accidental collisions potentially having EMR ratios exceeding the catastrophic threshold, only the Iridium-Cosmos collision resulted in a significant amount of fragmentation debris. This was likely due to non-central impact geometries and the structural characteristics of the objects involved. As a result, it was concluded that the critical impact cross-section leading to catastrophic collisions, especially for debris-intact events, might be significantly smaller than the overall impact cross-section.

As a result of this, an area scaling coefficient is proposed to assess the overestimation of catastrophic collisions. A simple model for assessing the probability of collision has been specifically applied to catastrophic events, considering three different collision scenarios: complete fragmentation of the parent objects, the generation of a significant population of large fragments due to an impact, and the creation of a significant population of large fragments resulting from an explosion triggered by an impact.

The implementation of the area scaling coefficient implies a linear change in the catastrophic collision rate and an almost linear change in the probability for low values, making it easily applicable.

The last chapter discusses various mitigation measures, all of which are necessary to prevent an increase in the current debris population. These four approaches include design improvements, disposal, active debris removal, and collision avoidance.
However, to comprehensively address the debris problem, there is a need to enhance detection and tracking capabilities for deploying countermeasures against debris in the 1-10 *cm* size range, where shielding and collision avoidance are not sufficient mitigation strategies. The implementation of an efficient collision avoidance system can prevent the majority of catastrophic collisions between intact objects and debris-intact objects, which are the primary contributors to the production of large collision debris populations.

Acronyms

L_c	Characteristic length
A/m	Area-to-Mass ratio
ADR	Active Debris Removal
ASAT	Anti Satellite Test
ASI	Agenzia Spaziale Italiana
DISCOS	Database and Information System Characterising Objects in Space
EMR	Energy-to-Mass Ratio
ESA	European Space Agency
GEO	Geostationary Orbit
HST	Hubble Space Telescope
LDEF	Long Duration Exposure Facility
LEGEND	LEO-to-GEO Environment Debris Model
LEO	Low Earth Orbit
MASTER	Meteoroid and Space Debris Terrestrial Environment Reference
MLI	Multi Layer Insulation
NASA	National Aeronautics and Space Administration
NORAD	North American Aerospace Defense Command

ODPO	Orbital Debris Program Office
PMD	Post Mission Disposal
PRIMA	Piattaforma Riconfigurabile Italiana Multi Applicativa
RORSAT	Radar Ocean Reconnaissance Satellites
SBM	Standard Breakup Model
SSN	Space Surveillance Network
TLE	Two Line Element set

References

[1] ESA Space Debris Office. *ESA'S ANNUAL SPACE ENVIRONMENT REPORT*. Tech. rep. 2023.

[2] Donald J Kessler et al. "The kessler syndrome: implications to future space operations". In: *Advances in the Astronautical Sciences* 137.8 (2010).

[3] NASA. "HANDBOOK FOR LIMITING ORBITAL DEBRIS". In: (2008).

[4] Carmen Pardini and Luciano Anselmo. "Evaluating the impact of space activities in low earth orbit". In: *Acta Astronautica* 184 (2021), pp. 11–22.

[5] Nicholas L Johnson et al. "NASA's new breakup model of EVOLVE 4.0". In: *Advances in Space Research* 28.9 (2001), pp. 1377–1384.

[6] Nicola Cimmino et al. "Tuning of NASA standard breakup model for fragmentation events modelling". In: *Aerospace* 8.7 (2021), p. 185.

[7] Martin Schimmerohn et al. "Numerical investigation on the standard catastrophic breakup criteria". In: *Acta Astronautica* 178 (2021), pp. 265–271.

[8] JC Dolado-Perez, Carmen Pardini, and Luciano Anselmo. "Review of uncertainty sources affecting the long-term predictions of space debris evolutionary models". In: *Acta Astronautica* 113 (2015), pp. 51–65.

[9] Carmen Pardini and Luciano Anselmo. "Review of past on-orbit collisions among cataloged objects and examination of the catastrophic fragmentation concept". In: *Acta Astronautica* 100 (2014), pp. 30–39.

[10] ESA. *Final Report Enhancement of S/C Fragmentation and Environment Evolution Models*. Tech. rep. Institute of Space Systems (IRAS), 2020.

[11] JC Liou et al. "Stability of the future LEO environment–an IADC comparison study". In: *Proceedings of the 6th European Conference on Space Debris*. Vol. 723. ESA. 2013.

[12] J.-C Liou et al. "LEGEND – a three-dimensional LEO-to-GEO debris evolutionary model". In: *Advances in Space Research* 34.5 (2004). Space Debris, pp. 981–986. ISSN: 0273-1177. DOI: https://doi.org/10.1016/j.asr.2003.02.027.

[13] Phillip Anz-Meador, John Opiela, and Jer-Chyi Liou. *History of on-orbit satellite fragmentations*. Tech. rep. 2023.

[14] ESA. *ESA's fragmentation database*. 2023. URL: https://fragmentation.esoc.esa.int/events.

[15] ESA. *ESA DISCOSweb*. 2023. URL: https://discosweb.esoc.esa.int/fragmentations.

[16] PD Anz-Meador and AE Potter. "Density and mass distributions of orbital debris". In: *Acta astronautica* 38.12 (1996), pp. 927–936.

[17] Gautam D Badhwar and Phillip D Anz-Meador. "Determination of the area and mass distribution of orbital debris fragments". In: *Earth, Moon, and Planets* 45.1 (1989), pp. 29–51.

[18] Donald J Kessler and Phillip D Anz-Meador. "Critical number of spacecraft in low Earth orbit: using satellite fragmentation data to evaluate the stability of the orbital debris environment". In: *Space Debris*. Vol. 473. 2001, pp. 265–272.

[19] Houman Hakima and Reza Emami. "Deorbiter CubeSat Mission Design". In: *Advances in Space Research* 67 (Jan. 2021). DOI: 10.1016/j.asr.2021.01.005.

[20] David A. Vallado et al. *Fundamentals of Astrodynamics and applications*. 4. ed. Space technology library. Hawthorne, CA: Microcosm press, 2013. ISBN: 9781881883197.

[21] James Mackey. "Recent US and Chinese antisatellite activities". In: *Air & Space Power Journal* 23.3 (2009), pp. 84–90.

[22] J-C Liou and NL Johnson. "Characterization of the cataloged Fengyun-1C fragments and their long-term effect on the LEO environment". In: *Advances in Space Research* 43.9 (2009), pp. 1407–1415.

[23] Luciano Anselmo and Carmen Pardini. "Analysis of the consequences in low Earth orbit of the collision between Cosmos 2251 and Iridium 33". In: *Proceedings of the 21st international symposium on space flight dynamics*. Centre nationale d'etudes spatiales Paris, France. 2009, pp. 2009–294.

[24] Carmen Pardini and Luciano Anselmo. "Physical properties and long-term evolution of the debris clouds produced by two catastrophic collisions in Earth orbit". In: *Advances in Space Research* 48.3 (2011), pp. 557–569.

[25] Lorenzo Olivieri and Alessandro Francesconi. "Large constellations vulnerability assessment". In: *population* 3 (2017), p. 4.

[26] Lorenzo Olivieri et al. "Fragments distribution prediction for ENVISAT catastrophic fragmentation". In: *8th European Conference on Space Debris, ESA/ESOC*. 2021, pp. 1–12.

[27] V Braun et al. "Operational support to collision avoidance activities by ESA's space debris office". In: *CEAS Space Journal* 8.3 (2016), pp. 177–189.

[28] F Covello et al. "COSMO-SkyMed an existing opportunity for observing the Earth". In: *Journal of Geodynamics* 49.3-4 (2010), pp. 171–180.

[29] Jason L Forshaw et al. "The active space debris removal mission RemoveDebris. Part 1: From concept to launch". In: *Acta Astronautica* 168 (2020), pp. 293–309.

[30] Guglielmo S Aglietti et al. "The active space debris removal mission RemoveDebris. Part 2: In orbit operations". In: *Acta Astronautica* 168 (2020), pp. 310–322.